Surface charge of single chain nanoparticles and protein adsorption

The effect of zwitterionic ligands on the formation of a protein corona

Jurriaan Sprik

Bachelor Thesis
BMT – Science and Technology
23-06-2021

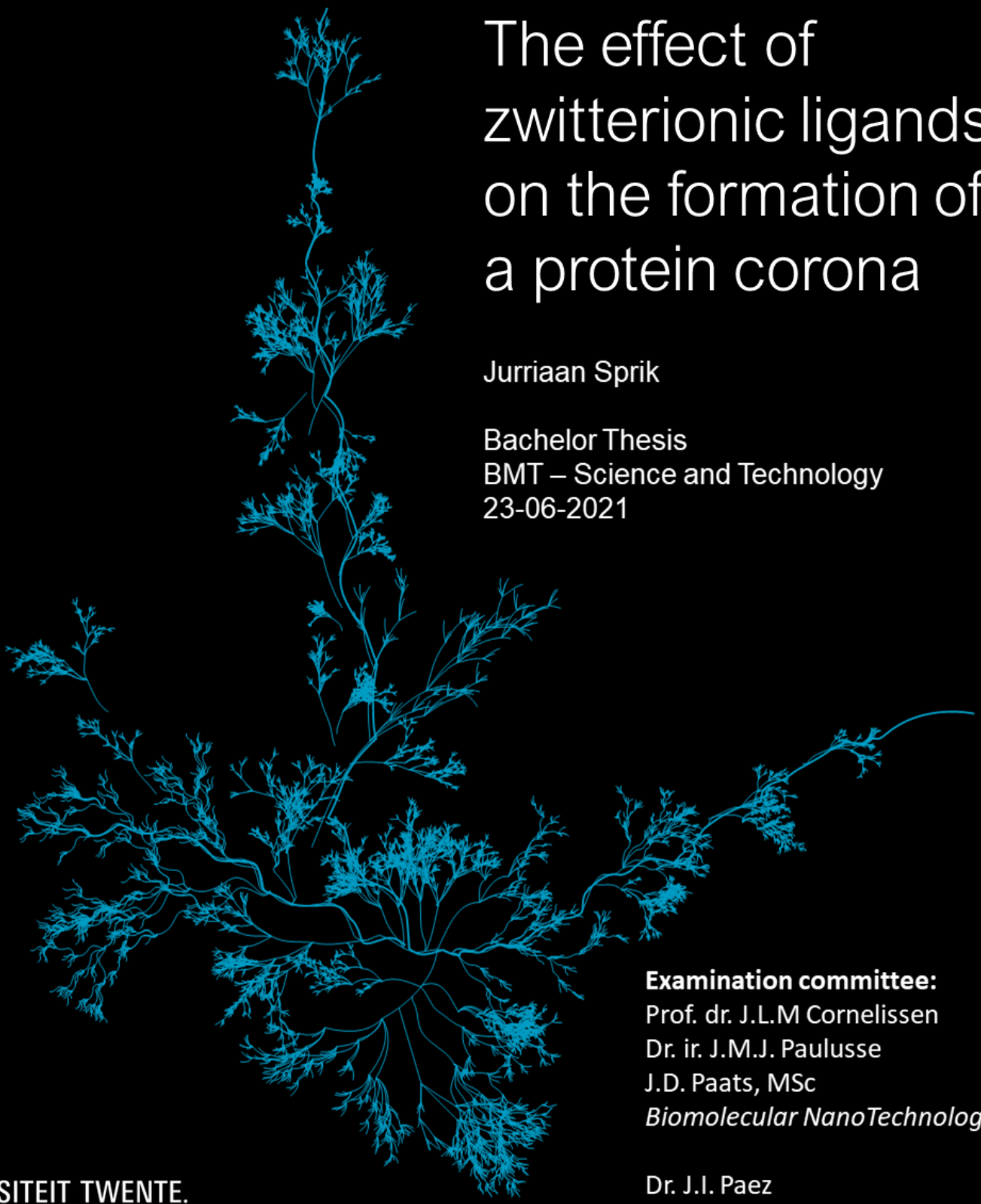

Examination committee:
Prof. dr. J.L.M Cornelissen
Dr. ir. J.M.J. Paulusse
J.D. Paats, MSc
Biomolecular NanoTechnology

Dr. J.I. Paez
Developmental BioEngineering

UNIVERSITEIT TWENTE.

Abstract

Single chain nanoparticles are an emerging field which show a lot of promise in drug delivery. Their intramolecular folding makes them extremely small compared to classic nanoparticles. In this thesis pentafluorophenyl copolymers will be crosslinked and functionalised with a zwitterionic amine (ADPS) and histamine, reaching conversions of 7, 16 and 21% for ADPS and 9, 20 and 23% for histamine. The nanoparticles were functionalised with ADPS for anti-fouling purposes, but was shown to increase the protein corona compared to a nanoparticle with only aminoglycerol groups. The nanoparticles were functionalised with histamine to research their tumour targeting properties, unfortunately the yield was too low to experiment with. The uptake and cytotoxicity of nanoparticles with ADPS ligands were analysed in HeLa and RAW 264.7 cell lines. The uptake of the nanoparticles increased with a higher percentage of ADPS ligands, and the RAW 264.7 cell line saw significantly more uptake than the HeLa cell line. The metabolic activity of both cell lines was increased 24 hours after addition of nanoparticles compared to controls showing no significant cytotoxicity. This research shows that particles with zwitterionic ligands are less effective than nanoparticles with aminoglycerol ligands at the prevention of a protein corona.

Samenvatting

Single chain nanoparticles is een opkomend veld waar veel toekomst in zit, vooral in het gericht afgeven van medicijnen. Hun intramoleculaire vouwing geeft ze een hele kleine grootte vergeleken met klassieke nanoparticles. In deze thesis worden pentafluorophenyl copolymeren gecrosslinked en gefunctionaliseerd met een zwitterionische amine (ADPS) en histamine. Er worden conversies verkregen van 7, 16 en 21% voor ADPS en 9,20 en 23% voor histamine. De nanoparticles zijn gefunctionaliseerd met ADPS voor anti-fouling eigenschappen, echter is gezien dat het voor de vorming van een grotere eiwit corona vergeleken met nanoparticles die alleen met aminoglycerol gefunctionaliseerd zijn. De nanoparticles zijn gefunctionaliseerd met histamine om het effect van tumor targeting te analyseren, helaas was hier de opbrengst hiervan te laag van om experimenten mee te doen. De opname en cytotoxiciteit van de deeltjes gefunctionaliseerd met ADPS zijn geanalyseerd in HeLa en RAW 264.7 cellijnen. De opname van de deeltjes nam toe met een groter percentage van ADPS liganden en de RAW 264.7 cellijn zag significant meer uptake dan de HeLa cellijn. De metabolische activiteit van beiden cellijnen was toegenomen in 24 na toevoeging van de deeltjes vergeleken met hun controles wat laat zien dat de deeltjes niet significant cytotoxisch zijn. Dit onderzoek laat zien dat deeltjes met zwitterionische liganden minder effectief zijn dat nanodeeltjes met aminoglycerol liganden in het voorkomen van het vormen van een eiwit corona.

Contents

1 Introduction

Nanomedicine is an incredibly fast-growing industry with an amazing breadth of applications and current research, from the controlled release of aspirin to specifically deliver chemotherapy medicine to tumour cells. [1, 2, 3] Nanomedicine consists of two parts: the medicine that eventually is supposed to enact change in the body, and the nanocarrier. An example of this is doxorubicin, the medicine, which is put into liposomes, the nanocarrier under the drug named Doxil. [4] The aim is for the particle to accumulate in tumour cells to increase efficacy and quality of life of the patient. It has been in production since 1995 and is used to great effect in solid tumours such as breast cancer, ovarian cancer and Kaposi's sarcoma caused by AIDS. [5, 6] The focus of this research will be on nanocarriers, also called nanoparticles.

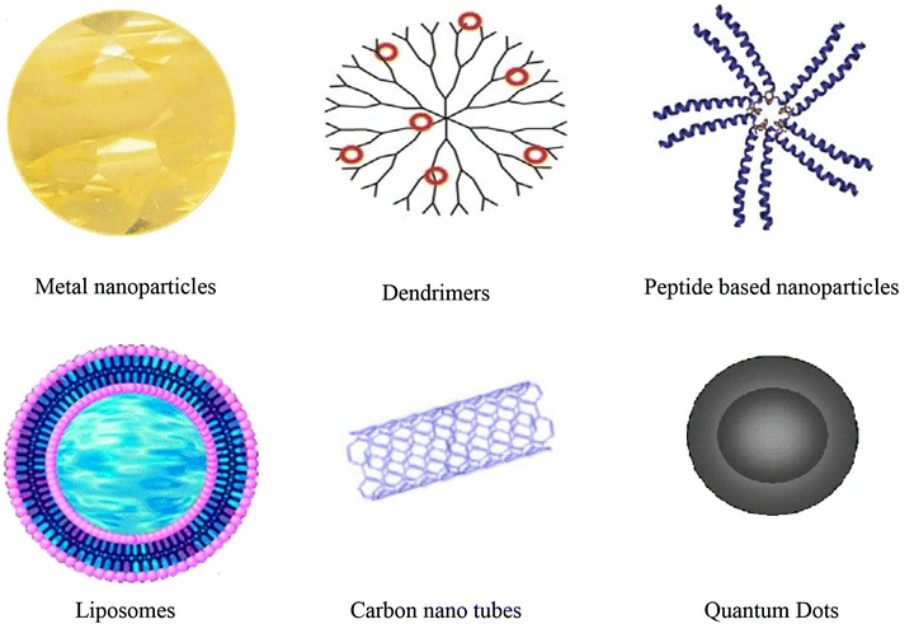

Figure 1: Different types of nanoparticles [1].

There are several different nanoparticles (figure 1), but they are all considered to be 10-1000 nm and subdivided in three categories: liposomal, polymeric, and inorganic nanoparticles. [7] Drugs are entrapped, dispersed, or surface adsorbed into or onto nanoparticles (figure 2). [7] However, nanoparticles face challenges in production and application. First, the body reacts efficiently to foreign bodies which can greatly affect the efficacy of the drug. [8] Second, nanoparticles are generally quite large on a bodily scale making it hard to squeeze into the places the medicine needs to reach. [9] Third, the functionalisation of smaller nanoparticles has been difficult to accurately control. [10] One of the biggest obstacles in the use of nanoparticles as drug delivery devices is the body itself, more specifically the innate defence, nanoparticles get removed from the blood stream or destroyed by this defence depending on many different factors. [8, 11, 12]

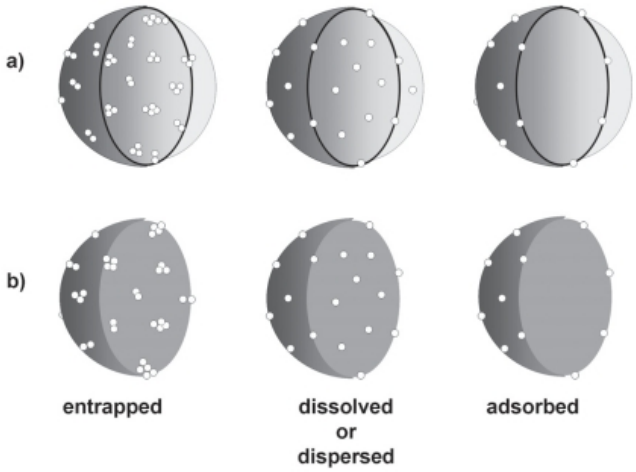

Figure 2: Drug entrapped, dispersed, and adsorbed into nanocapsules (a) and nanospheres (b) [13].

1.1 Innate defence

The innate defence of the body consists of many different factors that all are the first line of defence to invaders of the body, this rapport will focus on macrophages, neutrophils, dendritic cells since these are primarily responsible for cleaning up nanoparticles. [12, 14, 15] Macrophages are a monocyte-derived cell with receptors for carbohydrates not presented by normal human cells; if they detect these one of these structures they will encapsulate and destroy the attached particle. Neutrophils have extracellular traps that feel for and destroy foreign bodies from which inflammation generally results. Both neutrophils and macrophages have antigen and complement proteins, which can induce phagocytosis in microbes and signal for a larger immune response. Dendritic cells, as well as macrophages, are located near body surfaces where they clean up nanoparticles efficiently.

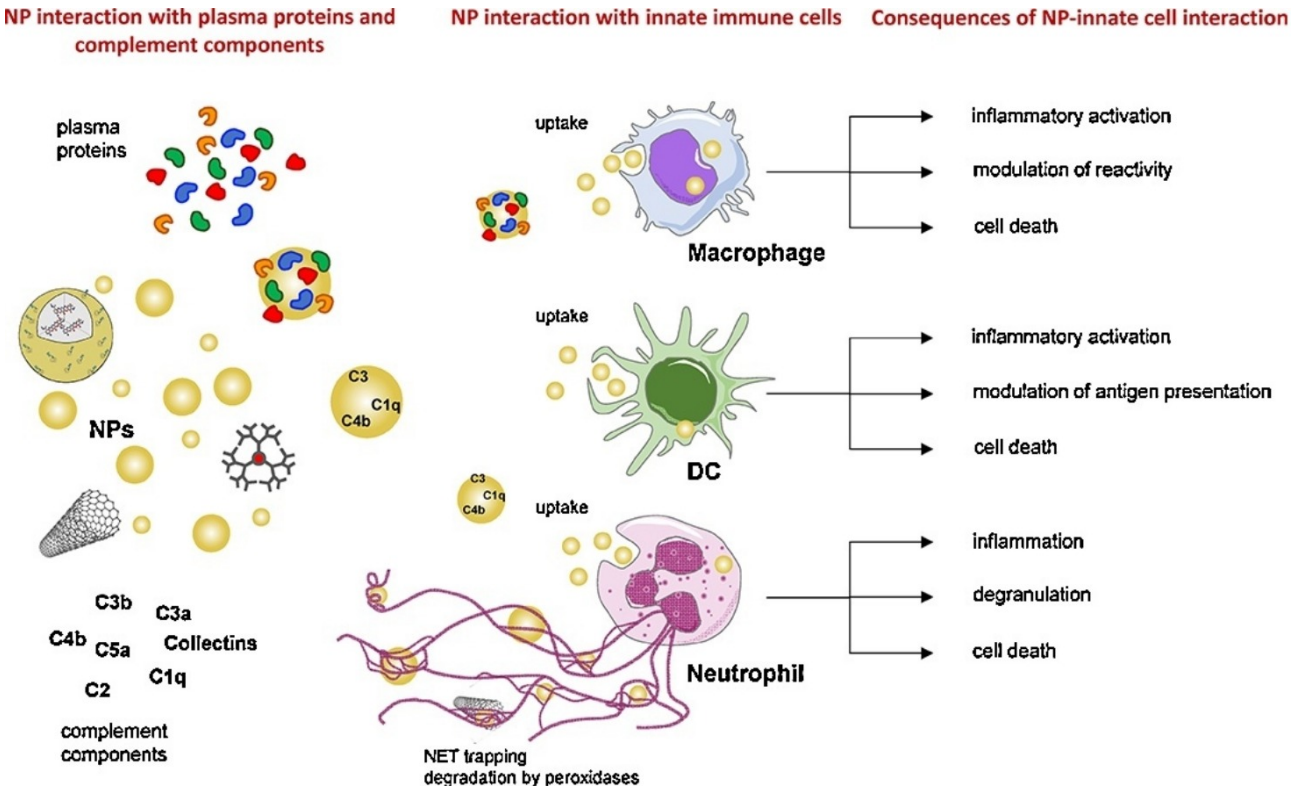

Figure 3: Overview of the innate immune system interaction with nanoparticles [12].

Depending on the size and shape of the nanoparticles, among other things, immune response already exists when nanoparticles enter the blood stream, but the greater problem arises when proteins and microbes from the blood stream adsorb on the nanoparticle, forming what is called the protein corona. [8] A greater protein corona decreases the uptake and increases the response of the immune system, which lowers circulation time. [16] There have been several strategies to prevent the formation of the protein corona, also called anti-fouling, with none being as widely used as PEGylation of the particle. [17] Unfortunately, physical reactions against PEG have surfaced. For example the allergic reaction and formation of anti-PEG. [17, 18] There have also been reports of PEG inhibiting cellular uptake and endosomal release. [19] Alternatives to PEG for preventing the formation of a protein corona seem to become a desirable research subject, in this thesis zwitterionic ligands will be researched as a possible alternative. In other papers, they have been found to have significant anti-fouling properties when attached to nanoparticles. [20, 21] Anti-fouling zwitterionic ligands have also been suggested as a suitable application in membranes. [22]

1.2 Tumour targeting

Cancer is arguably the biggest challenge that we currently face in medicine, in 2020 approximately 19.3 million people were diagnosed with cancer and approximately 10 million died due to cancer worldwide. [23] Treatment for most types of cancers still mostly consists of chemotherapy or other general treatment types, which are incredibly taxing on patients. [24] The next step in cancer research is to target tumour cells and deliver medicines specifically to these cells, increasing efficacy of the therapy and quality of living for cancer patients. [25] A field that is perfect for this application is nanomedicine and by extent nanoparticles. The niche that a tumour creates in the body is different in a few important ways, but mainly acidity. [26] The pH of a tumour niche lies around 6.5 compared to the normal pH of the body of 7.2-7.4, a good property to take advantage of. Nanoparticles with a positive surface charge see more uptake and cytotoxicity in non-phagocytic cells. Because of this ligands that protonate at pH 6.5 but have little to no protonation at pH 7.4 seem like good candidates (figure 4). [27, 28] When given enough circulation time particles with these properties will accumulate in tumours, where they can deposit their drug.

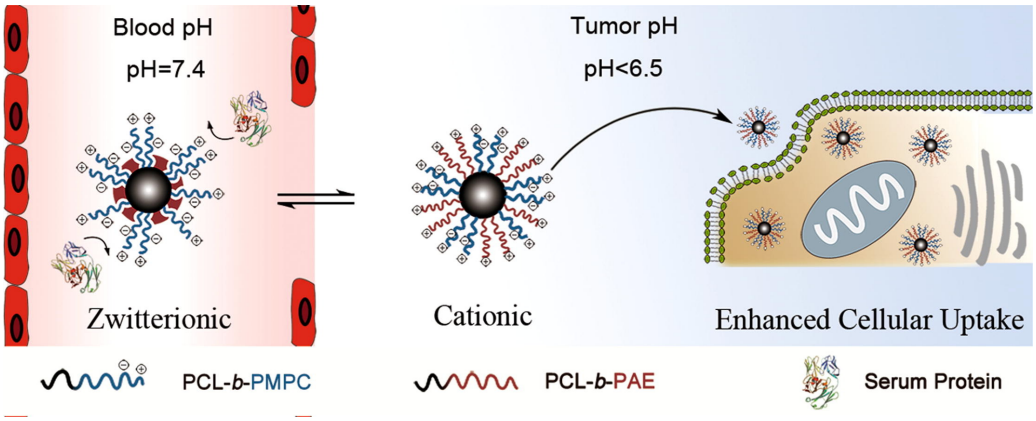

Figure 4: Visualisation of zwitterionic ligands which turn cationic [28].

1.3 Single chain nanoparticles

Size is one of the major properties of nanoparticles affecting the cytotoxicity, uptake, and immune reaction. [29] Regular nanoparticles are usually made in the range of 50-200 nm, but smaller is better since the uptake of a nanoparticle increases with a decrease in size. [30] Another deficiency of regular nanoparticles is the capability diffusing in the body, there have been reports that nanoparticles do not reach the cancer cells they are supposed to target due to their size. [9] One method of reaching a smaller size is a subtype of polymeric nanoparticles called single chain nanoparticles. These particles consist of a single polymeric backbone that, due to crosslinking, folds like a protein would, reaching possible sizes of 5-20 nm (figure 5). [31, 32] The first mention of single chain nanoparticles in literature was in 1962. [33] However, there have been issues with the production of these small nanoparticles, the crosslinking generally had to be done under harsh conditions and bringing low yields. [34] Fortunately, in 2002 Hawker et al. found a new way to synthesise single chain nanoparticles yielding relatively large amounts, by using continuous addition in production they practically reduced intermolecular crosslinking to zero. [35] They essentially scaled single polymer chain nanoparticle production up, opening a lot of doors for research and application. For example, drug delivery, [36], bionanoreactors [37], and imaging contrast agents. [38]

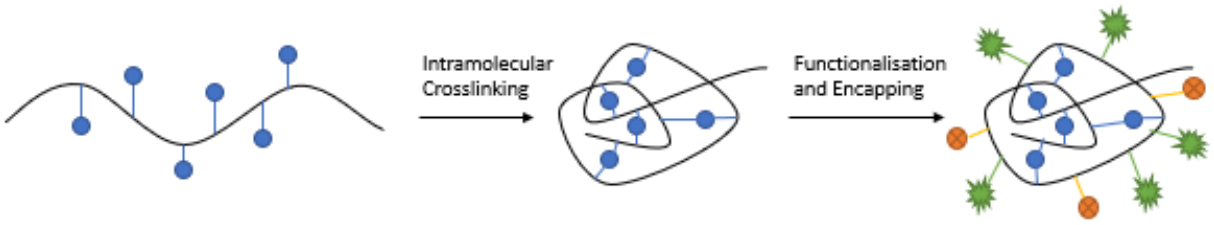

Figure 5: Visualisation of crosslinking and functionalisation of single chain nanoparticles.

1.3.1 Functionalisation

Another difficulty with these nanoparticles, however, is the controlled functionalisation with desired ligands. In the past multiple pathways to functionalisation have been found, but they had to be performed under undesirable conditions. For example, copper catalyzed functionalisation works quite well, but the usage of toxic metals make it difficult to use in biomedical applications; [39] functionalisations where potassium osmate has to be used, which is also quite toxic; [40] complicated conditions using EDC as a reactive agent have been used; [41] as well as harsh conditions which are needed for thiol-ene reactions. [42] Fortunately, in 2005 a polymer with pentafluorophenyl (PFP) ester groups was synthesised by Eberhardt et al. (figure 6). [43] Single chain nanoparticles that contain this PFP-ester polymer in their backbone can now be functionalised through amidation of the carbonyl next to the PFP-ester under more forgiving conditions, and this functionalisation can be quantified through ^{19}F NMR measurements comparing the free pentafluorophenol to the PFP-ester. [10, 32] These two properties give a relatively easy pathway, which is very well quantifiable, to functionalisation. This means that there are now single chain nanoparticles which are relatively easy to produce and functionalise, opening the way for starting a large and important field within nanomedicine.

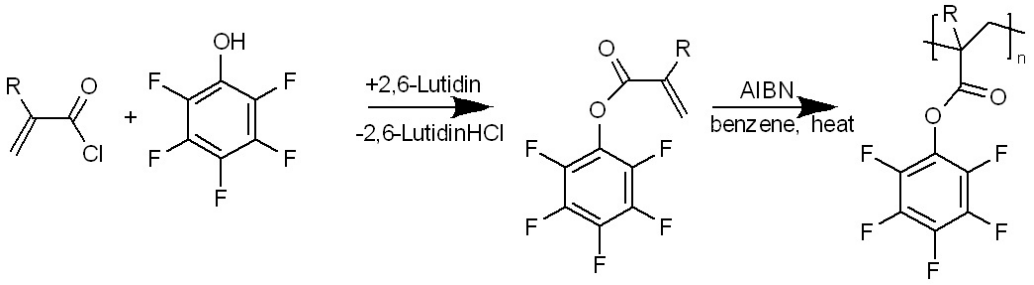

Figure 6: The synthesis of a PFP-functionalised backbone [43].

1.4 Aim of the research

In this thesis the focus will be placed on a possible replacement for PEG. A suitable candidate is the addition of a zwitterionic ligand, they will be chosen as a functionalisation of the single chain nanoparticles in this paper to research their impact. Histamine will also be researched as a ligand for the purposes of tumour targeting, due to its pKa of 6.0 it would be protonated partly around pH 6.5 and barely protonated around pH 7.4.

In this thesis, the production of single chain nanoparticles with 3-((3-aminopropyl)dimethylammonio)propane-1-sulfonate ligands at a target conversion of 10%, 20% and 30% will be researched. The anti-fouling effect of these ADPS ligands, as well as the effect they have on the uptake and viability in both HeLa and RAW 264.7 cell lines will be researched compared to particles with only aminoglycerol functionalisation. A pathway of production of single chain nanoparticles with histamine ligands with a target conversion of 10%, 30% and 50% will also be researched.

The nanoparticles will be labelled with DTAF fluorophore and analysed by gel permeation chromatography and dynamic light scattering. The protein corona formation will be analysed by separating the soft and hard corona and using SDS page to determine the size of the hard corona. The cell uptake will be qualitatively analysed through fluorescence microscopy and cytotoxicity will be analysed with an Alamar Blue assay.

2 Material and Methods

2.1 Synthesis of nanoparticles

The nanoparticles were crosslinked following the scheme in figure 7. [32] The crosslinkable pentafluorophenyl copolymer was supplied by J.D. Paats and synthesised according to the process described in the same article. [32]

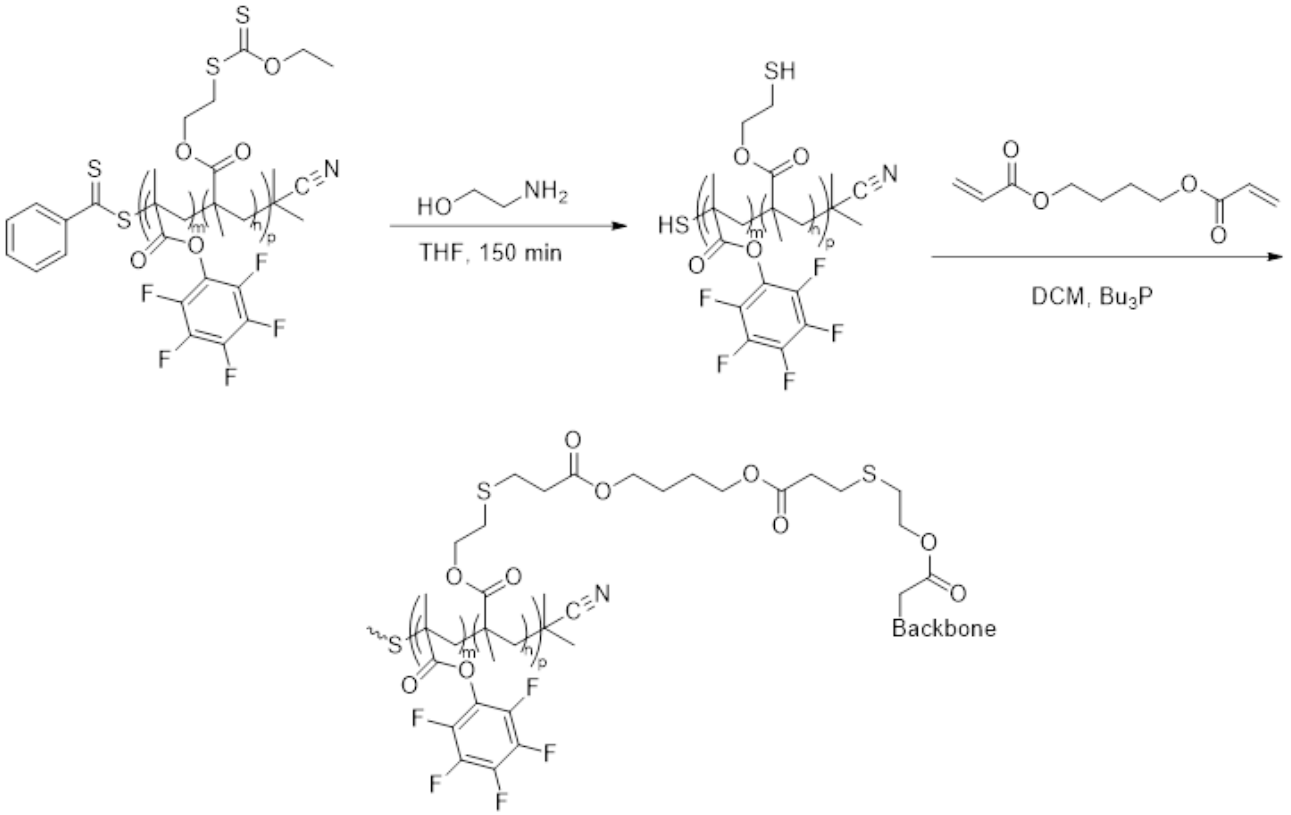

Figure 7: Reaction creating the nanoparticle and crosslinking. [32]

First, 600 mg of the PFP polymer was dissolved in 12 mL THF, this mixture was purged under nitrogen for 15 minutes after which ethanolamine was added. After this mixture was stirred for 2 hours, it was precipitated in 132 mL cold methanol and centrifuged at 10.000 rpm for 10 minutes. The precipitate was redissolved in 12 mL THF and added dropwise in a nitrogen purged mixture of 132 mL DCM, 45.20 μL 1,4 butanediol diacrylate, and 13 μL tributylphosphine. After everything was added, the mixture was stirred for 2 hours, then methyl acrylate was added as an endcapper and the mixture was stirred overnight. The mixture was dried under pressure and redissolved in 5 mL DCM, after which it was precipitated in cold methanol and centrifuged. This step was repeated once, after which the precipitate was left to dry. ^{1} H NMR (400 MHz, Acetone-d6) δ_H: 4.2 ($-COO-\mathbf{CH_2}-CH_2-S-$)), 3.6 ($-COO-\mathbf{CH_3}$), 3.3 ($-COO-(\mathbf{CH_2})^{\mathbf{3}}-$), 2.8 (crosslinker), 2.5 (backbone) ($-\mathbf{CH_2}-COO-$), 1.5 ($\mathbf{H}-S-$), 0.1 ($-\mathbf{CN}$). ^{19}F NMR (400 MHz, Acetone-d6) δ_F: -151.5, -159.7, -164.7.

2.2 Zwitterionic Amine

The zwitterionic amine was synthesised following the reacting scheme in figure 8 and a modified protocol. [44, 45]

tert-Butyl (3-(Dimethylamino)propyl)carbamate: The primary amine was protected by dissolving 7.41 gram N'N-dimethylaminopropylamine 72.5 mmol, 1 eq) in 38 mL methanol, cooling the solution to 0℃ and 15 gram adding di-tert-butyl dicarbonate (72.5 mmol, 1 eq). This mixture was left to stir overnight. Methanol was evaporated and the product was dissolved in 60 mL water. The product was extracted from the water with a 4x70 mL ethyl acetate wash, which was dried over magnesium sulphate. Finally, ethyl acetate was also evaporated, resulting in 9.6 gram tert-Butyl (3-(dimethylamino)-propyl)carbamate (47 mmol, 64% yield). ^{1} H NMR (400 MHz, CD_3Cl) δ_H: 5.1 (s), 3.63(s), 3.14 (s), 2.28 (2t, $-NH-\mathbf{CH_2}-CH_2-\mathbf{CH_2}-N-$), 2.18(s, $-N-(\mathbf{CH_3})^{\mathbf{2}}$), 1.60 (m, $-\mathbf{CH_2}-CH_2-N-$) , 1.4 ($(\mathbf{CH_3})^{\mathbf{3}}-C-O-$).

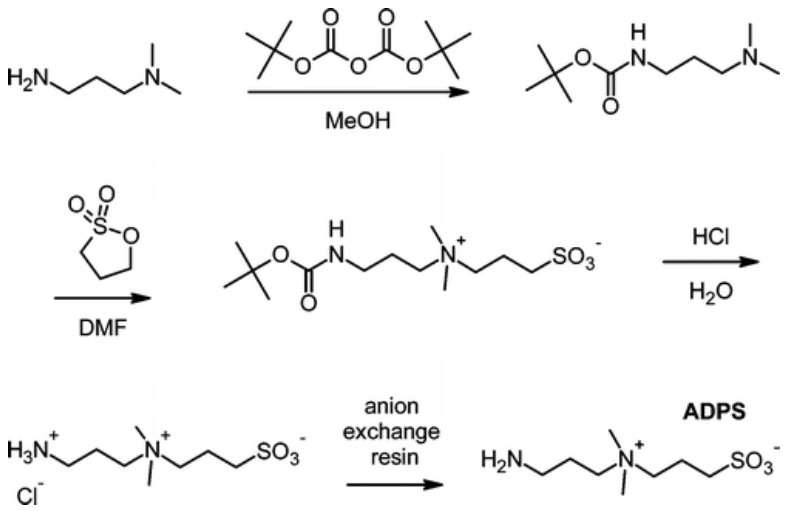

Figure 8: Creation of the zwitterionic amine. [44]

3-((3-((tert-Butoxycarbonyl)amino)propyl)dimethylammonio)propane-1-sulfonate: The tertiary amine was quaternized by mixing 9.6 grams tert-Butyl (3-(dimethylamino)-propyl) carbamate (47.4 mmol, 1 eq), 8.14 grams propane sultone (66.7 mmol, 1.4 eq) in 55.8 mL anhydrous N,N-Dimethylformamide (DMF), which was stirred for five days. After this the product was precipitated into 330 mL diethyl ether, which was centrifuged at 10 min x 10.000 rpm and dried under vacuum.

3-((3-Aminopropyl)dimethylammonio)propane-1-sulfonate-HCl (APDS-HCl): The product was used as such in the following step. It was deprotected by dissolving it in 100 mL DCM and adding 10 mL 4M HCl in dioxane, the product slowly precipitated. This mixture was stirred for 4 hours followed by filtration and washed with DCM and ethanol resulting 7.15 gram 3-((3-Aminopropyl)dimethylammonio)propane-1-sulfonate-HCl (27 mmol, 57% yield, based on the product of step 1)

3-((3-Aminopropyl)dimethylammonio)propane-1-sulfonate (ADPS): The final product was obtained by dissolving 2 gram 3-((3-Aminopropyl)dimethylammonio)propane-1-sulfonate-HCl (7.67 mmol) in water and adding an anion exchange resin (Amberlyst® A26 hydroxide) until pH > 12 was reached and was stirred for 4 hours. After filtering the mixture was freeze dried resulting in 1.7 gram 3-((3-Aminopropyl)dimethylammonio)-propane-1-sulfonate (7.57 mmol, 99% yield) ^{1} H NMR (400 MHz, D_2O) δ_H: 3.50, 3.40 (2 m, $-\mathbf{CH_2}-N^+(CH_3)_2-\mathbf{CH_2}-$), 3.13 (s, $-N^+(\mathbf{CH_3})_\mathbf{2}-$), 3.00 (t, $H_2N-\mathbf{CH_2}-$), 2.80 (t, $NH_2-\mathbf{CH_2}-CH_2-$), 2.23 (m, $NH_2-CH_2-\mathbf{CH_2}-$), 1.99 (m, $-\mathbf{CH_2}-CH_2-SO_3^-$).

2.3 Modification of nanoparticles

2.3.1 Zwitterionic modification

To modify the nanoparticles with ADPS ligands, 40 mg nanoparticle (0.139 mmol PFP-groups) was dissolved in 4 mL DMF at 50 ℃. 78 μL of triethylamine (4 eq) and the appropriate amount of ADPS was added (0.8 w/w% in propylene carbonate at 50 ℃). For 10% target conversion 5.8 mg (0.2 eq), for 20% 11.7 mg (0.4 eq), and for 30% 17.5 mg (0.6 eq) was added. After conversion was reached, 140 mg aminoglycerol (11 eq, 1.5 w/w% in DMSO) was added. When the full conversion was reached, the solution was placed in snakeskin 10k MWCO dialysis tubing, first against water with 20 g/L NaCl added, afterwards against clean water. The nanoparticles were freeze dried afterwards.

2.3.2 Histamine modification

To modify the nanoparticles with Histamine, 30 mg nanoparticle (0.104 mmol PFP-groups) was dissolved in 3 mL DMF at 50 ℃. 58 μL triethylamine (4 eq) was added and 11.7 mg ADPS (0.4 eq, 0.8 w/w% in propylene carbonate at 50 ℃) was added. After conversion was reached, the appropriate amount of histamine was added. For 10% target conversion 1.2 mg (0.1 eq), for 30% 3.5 mg (0.3 eq), and for 50% 5.8 mg (0.5 eq) was added. After conversion was reached, 140 mg aminoglycerol (11 eq, 1.5 w/w% in DMSO) was added. When the full conversion was reached, the solution placed in snakeskin 10k MWCO dialysis tubing, first against water with 20 g/L NaCl added, afterwards against clean water. The nanoparticles were freeze dried afterwards.

2.3.3 Control

For the control, the nanoparticles were only endcapped with aminoglycerol by dissolving 40 mg nanoparticle in 4 mL DMF and purging under nitrogen. 78 μL triethylamine (4 eq) and 140 mg aminoglycerol (11 eq, 1.5 w/w% in DMSO) was added. This was stirred overnight and analysed through F-NMR to measure conversion. When the full conversion was reached the solution placed in snakeskin 10k MWCO dialysis tubing, first against water with 20 g/L NaCl added, afterwards against dH_2O. The nanoparticles were freeze dried afterwards.

2.4 Fluorescent labelling

To correctly analyse the nanoparticles, fluorescent labelling was needed, which was done with 5-(4,6-Dichlorotriazinyl) aminofluorescein (DTAF) according to the reaction scheme in figure 9.

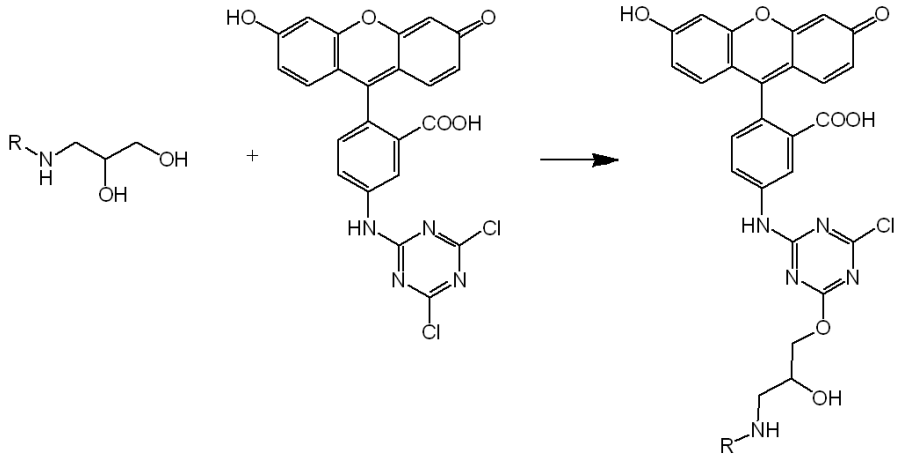

Figure 9: The reaction scheme for the fluorescent labelling of the nanoparticles, R is the rest of the nanoparticle.

In a typical experiment, 10 mg nanoparticle was dissolved in 2 mL sodium bicarbonate buffer and 0.499 mg DTAF (0.1 w/w% in DMSO) was added. This was supplemented to 2.5 mL total sodium bicarbonate and stirred overnight. This mixture was separated by PD10 column and the elution with the nanoparticle was freeze dried.

2.5 Characterisation of nanoparticles

The nanoparticles were analysed by gel permeation chromatography (GPC), nuclear magnetic resonance spectroscopy (NMR), and dynamic light scattering (DLS). Through GPC and DLS, the size of the nanoparticle can be analysed. DLS also measures the zeta potential, which gives feedback about the charge and stability of a nanoparticle. Both ^{1}H NMR and ^{19}F NMR were used to analyse the structure and measure the dissociation of PFP-groups respectively.

2.6 Protein corona formation

To analyse the effect that ADPS ligands have on the formation of a protein corona around the nanoparticles, labelled nanoparticles were incubated in cell culture medium (DMEM, 10% FBS, 1% pen/strep, 10 mM Glutamine) for two hours, after which they were centrifuged for 20 minutes at 15000 rpm and washed with 100 μL PBS to separate the hard corona and nanoparticle from the soft protein corona. The hard protein corona and nanoparticle were redissolved in 100 μL PBS. 30 μL of the nanoparticle/PBS solution was mixed with 10 μL 4x SDS-PAGE sample buffer (2.5 mL 1 M Tris-HCl pH 6.8, 0.5 mL of dH20, 1 g SDS, 0.8 mL 0.1% bromophenol Blue, 4 mL glycerol, 2 mL 14.3 M β-mercaptoethanol) of which 20 μL for each condition was added to the gel wells. The gel was attached to electrodes with a constant voltage of 150 volt and a target current of 15 mA in the stacking gel and 25 mA in the running gel. The control was done by following the same procedure as above, skipping the incubation in medium and starting from redissolving in 100 μL PBS. Both gels were fixed in fixing solution (50 v/v% ethanol, 10 v/v% acetic acid in dH_2O), after which they were stained for 30 minutes in Coumassie Blue staining solution (0.1 w/v% Coomassie blue R350, 20 v/v% ethanol, and 10 v/v% acetic acid in dH_2O). The gels were unstained using unstaining solution (50 v/v% ethanol, 10 v/v% acetic acid in dH_2O) until the background was clear again, after which the gels were allowed to enlarge again and stored in storage solution (5 v/v% acetic acid in dH_2O).

2.7 Cell experiments

The cell experiments were conducted on 96 well plates with a cell seeding density of 10^4 cells per well. All wells were cultured with the same medium (DMEM, 10% FBS, 1% pen/strep, 10 mM Glutamine). To analyse uptake, DTAF-labelled nanoparticles were added to the corresponding wells and they were incubated for 4 hours after addition. The cells were washed 2x with Hanks' Balanced Salt Solution (HBSS), fixated with 100 μL 4% paraformaldehyde, and incubated for 10 minutes. After this, they were washed with Phosphate Buffered Saline (PBS), incubating 10 minutes each time. The nucleus was stained by adding 50 μL DAPI stock (1/1000 v/v% in PBS) and the plate was incubated for 10 minutes. After the cells were washed again with PBS, 50 μL ActinRed (2 drops/mL PBS) was added and the plate was incubated again for 30 minutes. Finally, the cells were washed with PBS again and 100 μL PBS was added to prevent the cells from drying. The cells were analysed with fluorescence microscopy qualitatively and this same experiment was performed with an incubation time of 24 hours to analyse the longer term uptake. To analyse cytotoxicity, the cells were incubated for 24 hours after addition of nanoparticles. The medium was removed, 90 μL medium and 10 μL Alamar blue was added to each well and incubated for 4 hours, after which the emission was measured by a plate reader. The data was normalised to the positive control.

3 Results and Discussion

3.1 Synthesis of nanoparticles

The pentafluorophenyl single chain nanoparticle was created by deprotecting the copolymer through reacting with ethanolamine in THF creating a free thiol, which can be seen with the disappearance of the peak at 4.6 ppm and the appearance of a peak at 4.0 ppm in the ^{1}H NMR (figure 10).

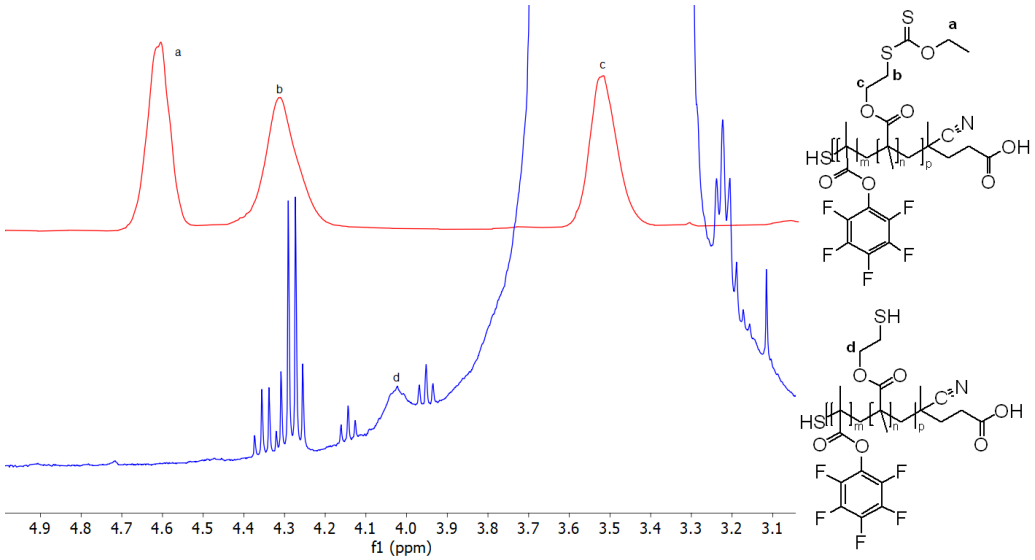

Figure 10: ^{1}H NMR of deprotected PFP-copolymer (above) and original copolymer (below).

Next, the nanoparticle was crosslinked by slowly adding it to a butanediol diacrylate mixture, after which it was endcapped with methyl acrylate. This can be seen with the disappearance of peaks at 4.6, 4.3, and 3.5 ppm, and the appearance of peaks at 4.2, 3.6, and 3.3 ppm in the ^{1}H NMR (figure 11).

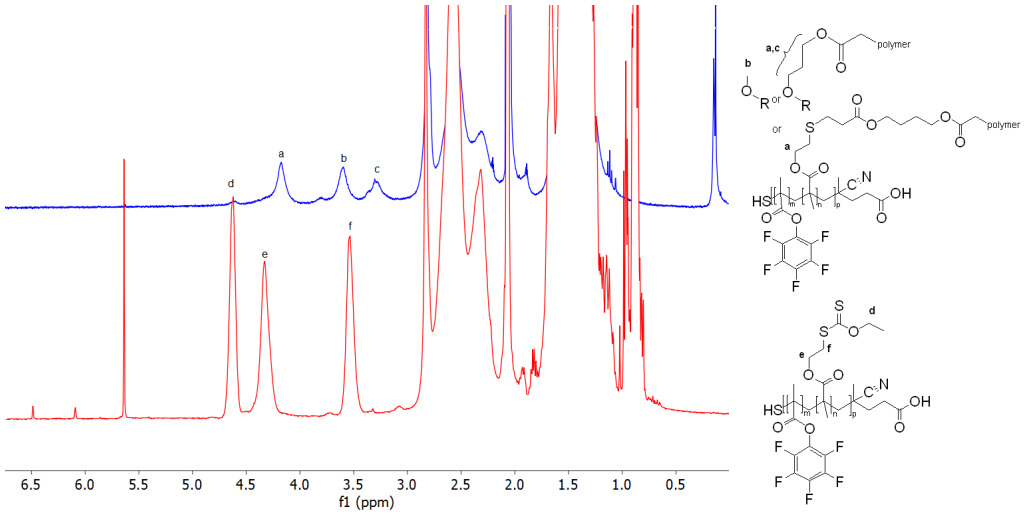

Figure 11: ^{1}H NMR comparison of PFP-SCNP (above) and PFP-copolymer (below).

The original and the resulting crosslinked single chain nanoparticle were analysed with GPC. The elution time of the nanoparticle has increased after crosslinking (figure 12) and the crosslinked nanoparticle has a polydispersity index of 1.7 compared to the 1.5 of the original polymer. This indicates that nanoparticle became smaller than the original polymer with

the crosslinker, but did not uniformly crosslink. Through ^{19}F NMR no degradation of the PFP-groups was observed (Appendix, figure 27 and 28).

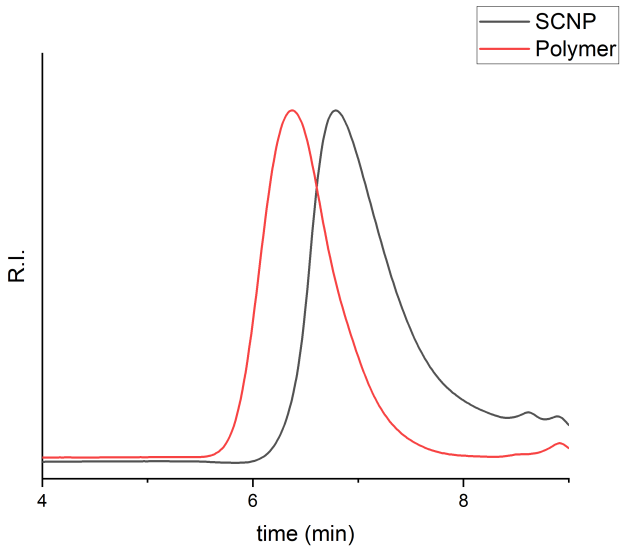

Figure 12: Gel permeation chromatography elution graph of the crosslinked nanoparticle (SCNP) and the original copolymer.

3.2 Zwitterionic Amine

To synthesise ADPS, the primary amine of N'N-dimethylaminopropylamine was protected with di-tert-butyl dicarbonate while the quarternisation of the tertiary amine with propane sultone was completed, resulting in a viscous liquid. After deprotection of the primary amine with HCl, ADPS-HCl was treated with an anion exchange resin to produce ADPS. After this step, you can see a clear separation of the ^{1}H NMR peaks around 3.4, 2.9, and 2.2 ppm (figure 13).

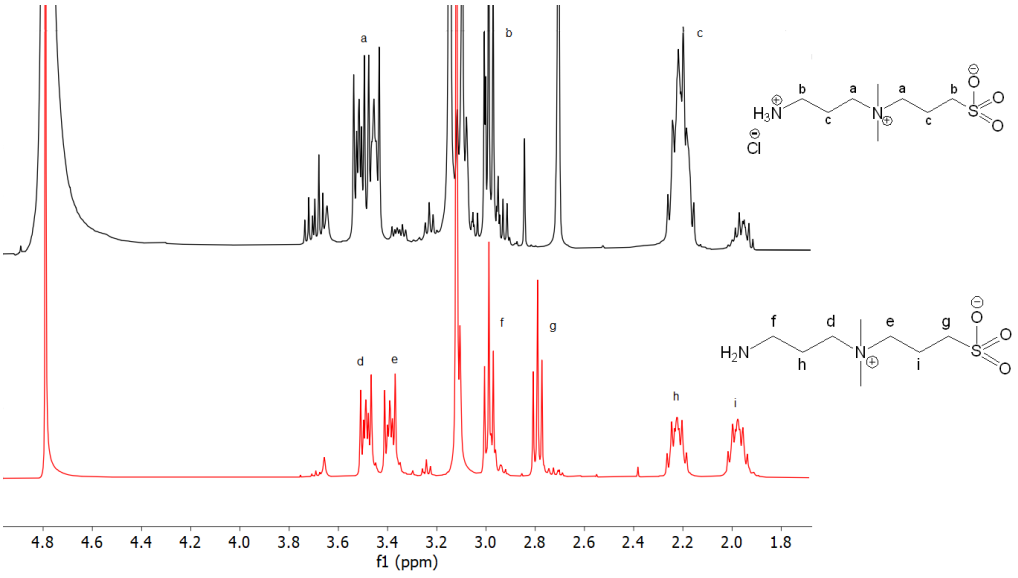

Figure 13: ^{1}H NMR comparison of ADPS (above) and ADPS-HCl (below).

3.3 Modification of nanoparticles

In general, all modification experiments followed the same steps, as described in section 2. All ^{19} F NMR spectra used for the determination of conversion in the modification experiments can be found in the appendix, as well as all ^{1}H NMR graphs.

3.3.1 Zwitterionic modification

ADPS was quite insoluble in organic solvents, because of this propylene carbonate at 50℃ was chosen from literature as the solvent. [44] The conversion (table 1) was lower than expected for each equivalent, which could have been caused by steric hindrance due to the size of ADPS, or by the polarity of the molecule, both making reactions more difficult. By adding double of the intended equivalent a conversion nearing the desired percentages was reached. However, an accurate estimation of conversion is possible, through ^{19}F NMR analysis (example of 0.4 eq ADPS in figure 14) and afterwards endcapping with 11 equivalent aminoglycerol.

Table 1: Modification with ADPS.

Target conversion (%)	Actual conversion (%)	eq
10	7	0.2
20	16	0.4
30	21	0.6

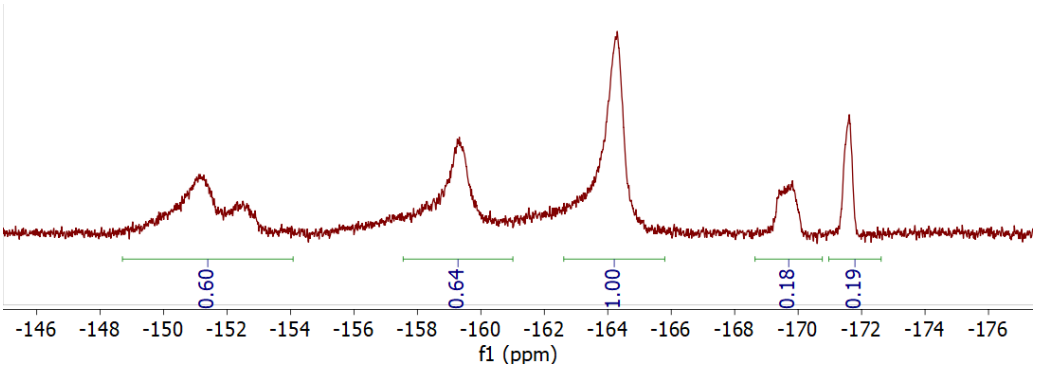

Figure 14: Determination of the conversion by ADPS (eq 0.4) with ^{19}F NMR (0.19/1.19 = 15.6%).

The control and all the conversions with ADPS were analysed through gel permeation chromatography to give an indication of size and polydispersity index. The control, only modified with aminoglycerol, was a smooth graph which is expected. However, in the graph of the nanoparticles modified with ADPS a bump is visible around 8 minutes and 40 seconds. This means that the nanoparticles modified with ADPS had larger sizes besides the main peak, which implies aggregation of the nanoparticles with ADPS ligands. This could be caused by the polarity of the ADPS ligands or entanglement due to the length of the ligands.

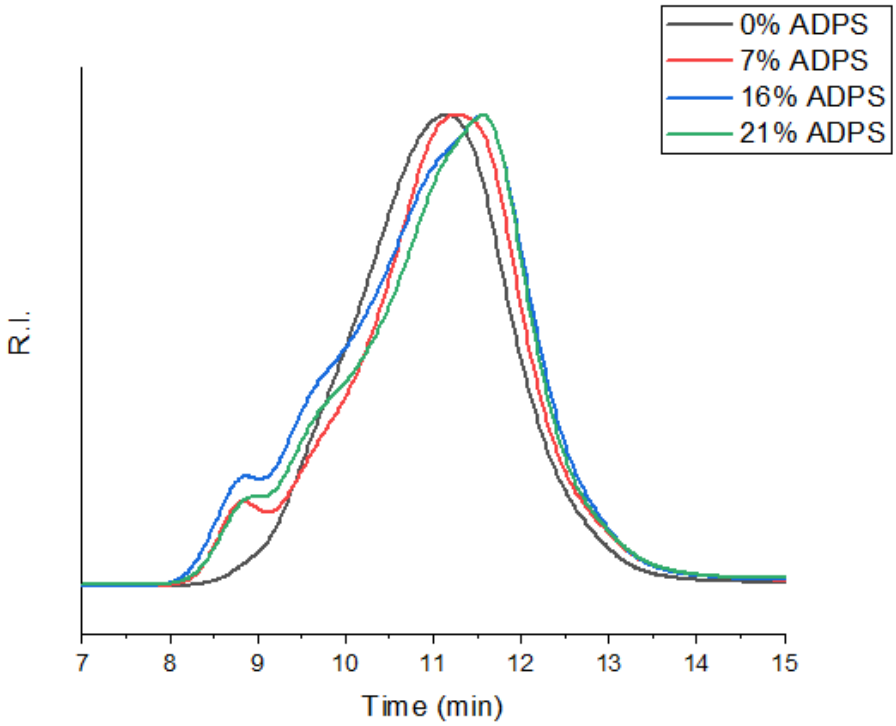

Figure 15: Gel permeation chromatography graph of the control and different conversions with ADPS.

These particles were also analysed by a zetasiser DLS machine, with which the size and zeta potential were determined (figure 16, table 2). In all particles with ADPS ligands aggregation is visible, in all but 7% ADPS nanoparticle the second peak is around 7 times larger at a non-negligible 20% of the mass. The 7% ADPS nanoparticle shows only one peak around 169.2 nanometre which also points to aggregation. The control nanoparticle with 0% ADPS ligands shows a peak around 516.2 nm, but this is a negligible 0.5% of the mass. The zeta potential increases with each nanoparticle, which is expected due to the outward facing negatively charged sulfonate group that is added with the ADPS ligands. From this it can be concluded that the ADPS ligands make the particle more likely to aggregate, which presents problems for their application in nanomedicine.

Table 2: Size (diameter nanometre), zeta potential (mV), and polydispersity index provided by DLS.

Particle	Size peak 1 (d.nm)	% Mass 1	Size peak 2 (d.nm)	% Mass 2	Zeta potential (mV)	Polydispersity index
0% ADPS	22 ± 9	99.5	516 ± 285	0.5	-23	0.6
7% ADPS	169 ± 82	100	0 ± 0	0	-29	0.3
16% ADPS	34 ± 10	76	237 ± 112	24	-30	0.3
21% ADPS	39 ± 16	83	253 ± 113	17	-29	0.5

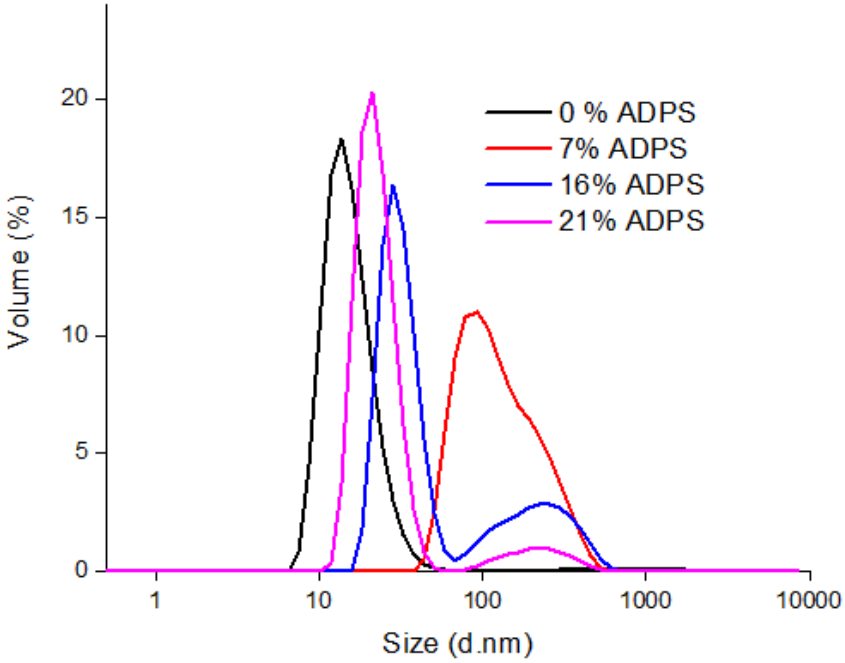

Figure 16: DLS results graph of the volume (%) against the size.

3.3.2 Histamine modification

Histamine modification did not go flawlessly. While it was easily soluble in DMF, the mixture was still kept at 50℃ due to the nanoparticle also first being modified with ADPS. When the nanoparticles were endcapped and placed in dialysis bags, however, they precipitated even under acidic conditions. The yield was around 1 mg, which was not enough to perform experiments with. An exploration into another way of fabrication could be a further avenue of research into these particles. Again, the conversion (table 3) was lower than expected and when adding 0.5 eq histamine it became apparent that reaching higher conversions than 20% is difficult (figure 17). This could be a result of the nanoparticle becoming less soluble as more histamine gets added, affecting the measurements as well as the reaction. The recommendation for further research is improving the solubility of the molecule, hopefully increasing yield. Furthermore, due to the abnormally low yield, follow-up research could entail starting with a larger amount of single chain nanoparticles to produce a yield with which experiments are possible.

Table 3: Modification with histamine, adjusted for 15% conversion with ADPS first.

Target conversion (%)	Actual conversion (%)	eq
10	9	0.1
30	20	0.3
50	23	0.5

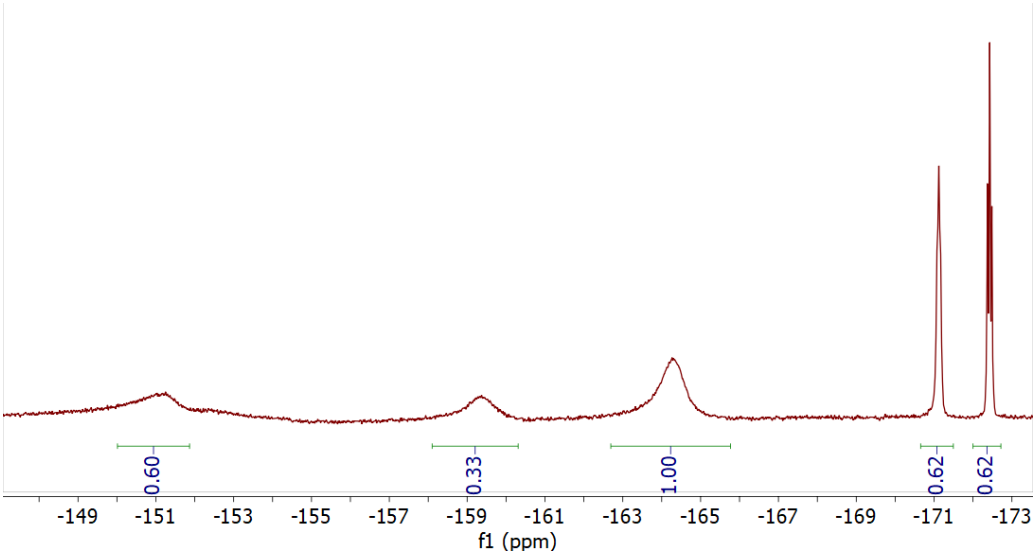

Figure 17: Determination of the conversion by Histamine (eq 0.3) with ^{19}F NMR (0.62/1.62 = 38.2% - 15%, thus 23% conversion).

3.4 Protein corona formation

In the SDS-PAGE run (figure 18), denatured proteins are visible in every lane, which means that a protein corona does still form around each nanoparticle. The bands represent the denatured proteins of each protein corona. The nanoparticle sample with 0% ADPS has the lowest intensity, meaning that there was a smaller protein corona around that nanoparticle compared to the others. Between the nanoparticles with ADPS ligands, there is no big difference in intensity, although the 25% seems to be slightly smaller. This indicates that an increase of ADPS ligands decreased the anti-fouling of the nanoparticle compared to a nanoparticle with only aminoglycerol ligands. In other studies, glycerol has been used as an anti-fouling agent successfully. [46, 47] There has also been a comparison study where hydrophilic anti-fouling performed better than zwitterionic anti-fouling. [48] According to this experiment glycerol is a better anti-fouling ligand than zwitterionic ligands as well. A control experiment where the nanoparticles were dissolved in PBS and run through a SDS-PAGE gel gave little to no signal (figure 19). Thus it can be concluded that most of the signal in figure 18 is from the protein coronas of their respective nanoparticles. Further analysis of the protein corona, with for example a protein quantification assay, is necessary to determine a true quantifiable difference in the formation of protein coronas around these nanoparticles.

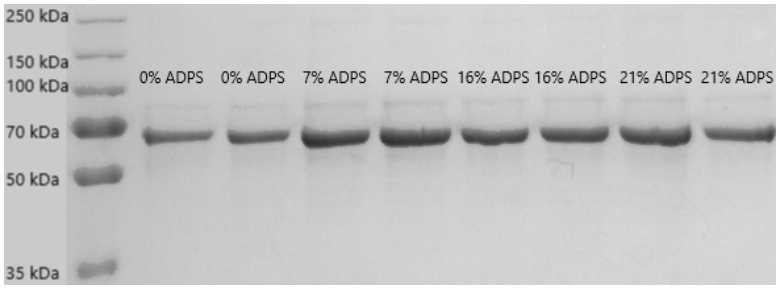

Figure 18: Photo of the SDS-PAGE gel run of nanoparticles incubated with medium (DMEM, 10% FBS, 1% pen/strep, 10 mM Glutamine) in PBS.

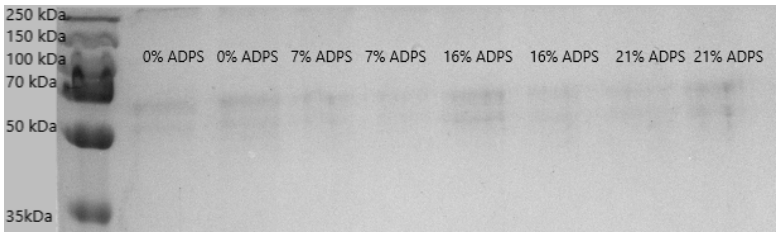

Figure 19: Photo of the SDS-PAGE gel run of unincubated nanoparticles in PBS.

3.5 Cell experiments

3.5.1 Uptake

In all cell experiments more signal was visible in the RAW 264.7 cell line than in the HeLa cell line (figure 20, 21, 22, 23). There was little to no DTAF signal in HeLa cell lines after 4 hours of incubation. 15% and 25% ADPS nanoparticles did see a bit more signal, however these seem to be disjointed from cell staining and are presumed to be nanoparticles that have aggregated together and could not be washed away. However, after 24 hours there is more signal with correlation to cell staining, especially of the 0% ADPS nanoparticles (figure 20), which indicates increased uptake compared to 4 hours. The amount of signal also increases with more ADPS ligands, which is presumed to be a mix of more uptake and aggregation due to the zwitterionic properties and which was also visible at shorter incubation times. The RAW 264.7 cell lines signal is visible in every experiment and those signals strongly correlate with cell staining, which indicates a lot of uptake. This is expected as macrophages are cells that specifically clean up foreign bodies. This uptake increases with time, as well as with percentage of ADPS ligands. From this, it can be concluded that the amount of ADPS ligands certainly has an effect on the uptake in RAW 264.7 cell line. The signal seen in the HeLa cell line could either be due to uptake or aggregation. Either way the signal is significantly less than in the RAW 264.7 cell line, which is as expected because is there no active reason for the HeLa cells to take the nanoparticles up. More detailed analysis with, for example confocal laser scanning microscopy or fluorescence-activated cell sorting is needed in order to provide clarification and quantification of the amount of uptake in each cell line.

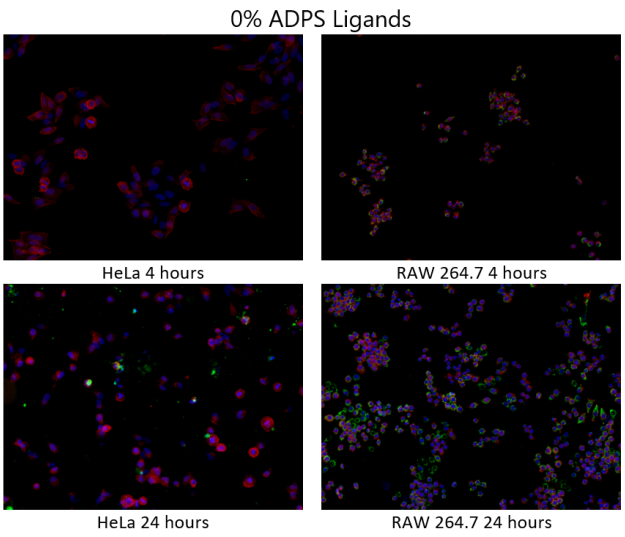

Figure 20: The uptake of 0% ADPS nanoparticles in HeLa (left) and RAW 264.7 (right) cell lines after 4 (above) and 24 (below) hours.

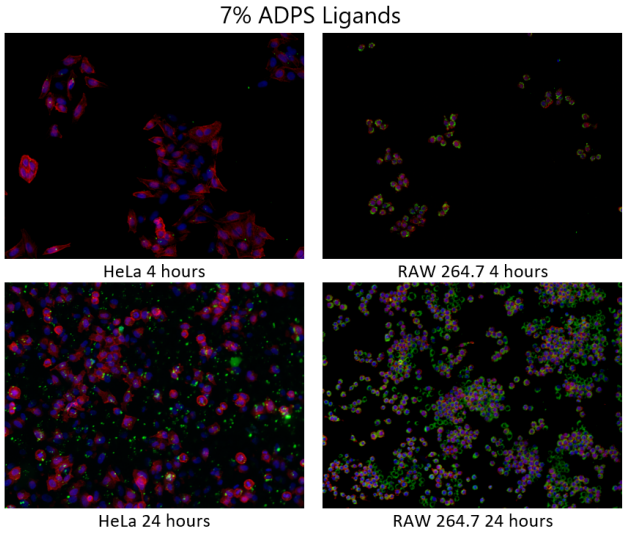

Figure 21: The uptake of 7% ADPS nanoparticles in HeLa (left) and RAW 264.7 (right) cell lines after 4 (above) and 24 (below) hours.

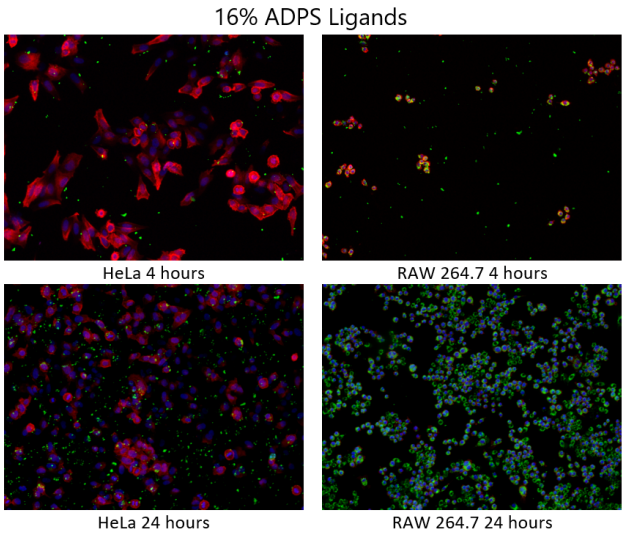

Figure 22: The uptake of 16% ADPS nanoparticles in HeLa (left) and RAW 264.7 (right) cell lines after 4 (above) and 24 (below) hours.

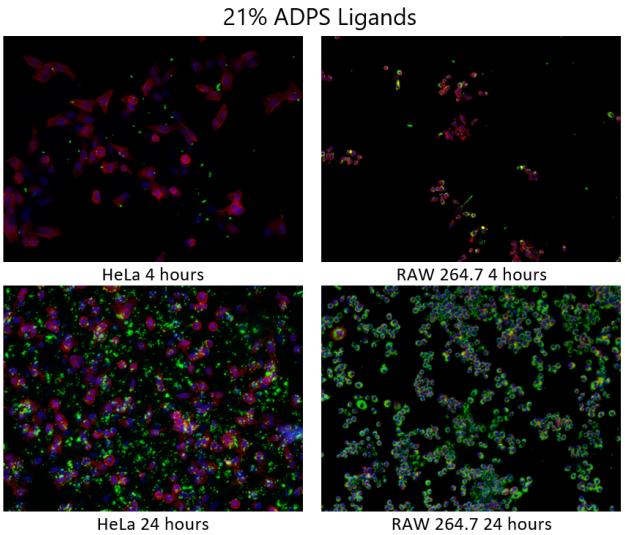

Figure 23: The uptake of 21% ADPS nanoparticles in HeLa (left) and RAW 264.7 (right) cell lines after 4 (above) and 24 (below) hours.

3.5.2 Viability

The viability assay (figure 24) showed that, in general, the metabolic activity of both cell lines increased with the addition of nanoparticles, which could be caused by breaking down the nanoparticles. The RAW 264.7 cell line saw significantly more metabolic activity compared to its control than HeLa cells, which could be caused by being activated and trying to take up and destroy the nanoparticles. From both cytotoxicity assays, it can be assumed that the particles are not cytotoxic, due to seeing strong activity of both cell lines after 24 hours of addition. This indicates that the nanoparticles are suitable for use in medical applications. The negative controls were incubated with isopropanol for 24 hours instead of medium, this shows the resilience of the RAW 264.7 cell line.

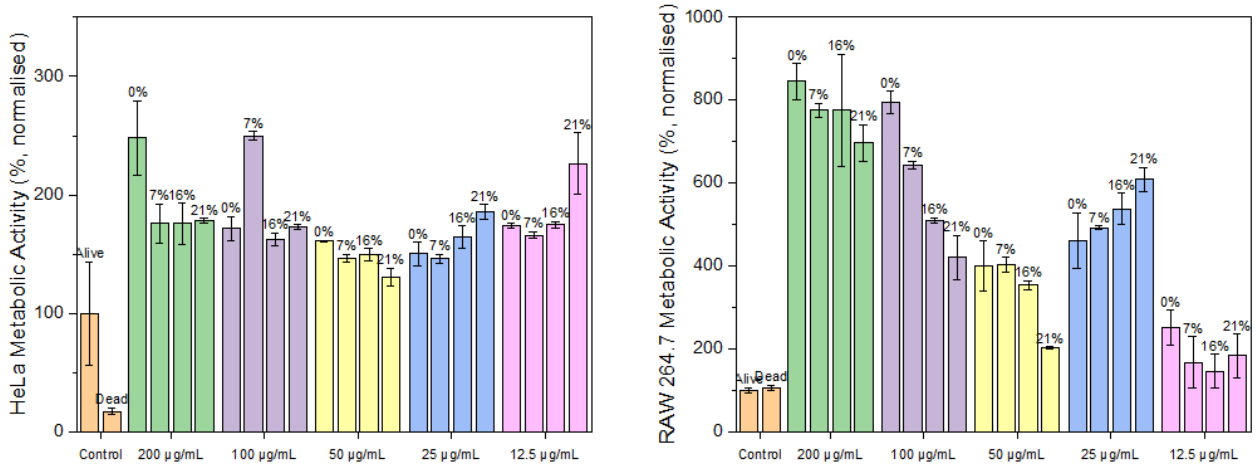

Figure 24: Viability Assay of HeLa cells (left) and RAW 264.7 cells (right), normalised to the control. Percentages amount of PFP groups converted to ADPS on the single chain nanoparticle.

4 Conclusions

In this thesis the effectiveness of modification of pentafluorophenyl single chain nanoparticles with histamine and 3-((3-Aminopropyl)dimethylammonio)propane-1-sulfonate (ADPS), as well as the effect of the zwitterionic ADPS ligands on the formation of a protein corona and their effect on cells, was demonstrated. The functionalisation of the single chain nanoparticles with ADPS was successfully completed, albeit with lower conversion than was targeted. The functionalisation of the single chain nanoparticles with histamine was also achieved with a lower conversion than expected and with a significantly lower yield than anticipated, unfortunately making cell experiments impossible. The effect of ADPS ligands on the formation of a protein corona was unexpected, the addition of ADPS ligands seemed to allow a larger protein corona to form making the endcap of aminoglycerol more effective at the prevention of a protein corona. This result opens the door to easier anti-fouling by using less complicated structures as anti-fouling ligands, since aminoglycerol is both easier to produce and to attach to a nanoparticle. The ADPS ligands make the nanoparticle more likely to aggregate, presumably due to steric and polarisation effects. The effect of ADPS ligands on the uptake is inconclusive: more signal has been seen with higher percentages of ADPS ligands after washing, but this could also be because of aggregation due to the affinity of zwitterionic ligands. The cytotoxicity assay showed higher metabolic activity in the cells with nanoparticles added than in wells without nanoparticles added after 24 hours. Thus the nanoparticles are not cytotoxic and can be used in biomedical applications. It is recommended to perform further into another anti-fouling method, since the ADPS ligands make a particle more likely to aggregate and has less anti-fouling effects than glycerol. It would also be recommended to research making histamine particles more agreeable, or performing research into another targeting functionalisation. Further research into these nanoparticles and possible other functionalisation thereof is certainly required due to the applications in this field.

5 Acknowledgements

My sincerest gratitude to J.D. Paats, MSc; N.M. Hamelmann, MSc; Drs.ing. R.M. van der Hee; M.A.J. de Bruine and Dr. ir. J.M.J. Paulusse for their daily support and advice in my experiments. Furthermore, I would like to extend my special thanks to Prof. dr. J.J.L.M Cornelissen, Dr. J.I. Paez, Ing. B.H.M. Ruel, and Ing. Richard J. M. Egberink.

References

[1] Mirza, A. Z. & Siddiqui, F. A. Nanomedicine and drug delivery: a mini review. *International Nano Letters* **4** (2014).

[2] Shi, Y., Wan, A., Shi, Y., Zhang, Y. & Chen, Y. Experimental and mathematical studies on the drug release properties of aspirin loaded chitosan nanoparticles. *BioMed Research International* **2014**, 1–8 (2014).

[3] Rosenblum, D., Joshi, N., Tao, W., Karp, J. M. & Peer, D. Progress and challenges towards targeted delivery of cancer therapeutics. *Nature Communications* **9** (2018).

[4] Duggan, S. T. & Keating, G. M. Pegylated liposomal doxorubicin. *Drugs* **71**, 2531–2558 (2012).

[5] Barenholz, Y. C. Doxil® — the first fda-approved nano-drug: Lessons learned. *Journal of Controlled Release* **160**, 117–134 (2012).

[6] Cancer, C. C. Doxil ®. URL `https://chemocare.com/chemotherapy/drug-info/doxil.aspx`.

[7] Mohanraj, V. J. & Chen, Y. Nanoparticles - a review. *Tropical Journal of Pharmaceutical Research* **5** (2007).

[8] Wani, T. U., Raza, S. N. & Khan, N. A. Nanoparticle opsonization: forces involved and protection by long chain polymers. *Polymer Bulletin* **77**, 3865–3889 (2019).

[9] Peng, J. *et al.* Tumor microenvironment responsive drug-dye-peptide nanoassembly for enhanced tumor-targeting, penetration, and photo-chemo-immunotherapy. *Advanced Functional Materials* **29**, 1900004 (2019).

[10] Gruber, A., Navarro, L. & Klinger, D. Reactive precursor particles as synthetic platform for the generation of functional nanoparticles, nanogels, and microgels. *Advanced Materials Interfaces* **7**, 1901676 (2019).

[11] Liu, Y., Hardie, J., Zhang, X. & Rotello, V. M. Effects of engineered nanoparticles on the innate immune system. *Seminars in Immunology* **34**, 25–32 (2017).

[12] Boraschi, D. *et al.* Nanoparticles and innate immunity: new perspectives on host defence. *Seminars in Immunology* **34**, 33–51 (2017).

[13] Guterres, S. S., Alves, M. P. & Pohlmann, A. R. Polymeric nanoparticles, nanospheres and nanocapsules, for cutaneous applications. *Drug Target Insights* **2**, 117739280700200 (2007).

[14] Delves, P. J. & Roitt, I. M. The immune system. *New England Journal of Medicine* **343**, 37–49 (2000). URL `https://doi.org/10.1056/NEJM200007063430107`. PMID: 10882768, `https://doi.org/10.1056/NEJM200007063430107`.

[15] Marieb, E. N. & Hoehn, K. *The Immune System: Innate and Adaptive Body Defenses*, 791–826 (Pearson Education Limited, 2016), 10 edn.

[16] Anderson, J. M., Rodriguez, A. & Chang, D. T. Foreign body reaction to biomaterials. *Seminars in Immunology* **20**, 86–100 (2007).

[17] Zhang, F., Liu, M.-R. & Wan, H.-T. Discussion about several potential drawbacks of pegylated therapeutic proteins. *Biological and Pharmaceutical Bulletin* **37**, 335–339 (2014).

[18] Cox, F., Khalib, K. & Conlon, N. Peg that reaction: A case series of allergy to polyethylene glycol. *The Journal of Clinical Pharmacology* **61**, 832–835 (2021).

[19] Hatakeyama, H., Akita, H. & Harashima, H. The polyethyleneglycol dilemma: Advantage and disadvantage of pegylation of liposomes for systemic genes and nucleic acids delivery to tumors. *Biological and Pharmaceutical Bulletin* **36**, 892–899 (2013).

[20] Debayle, M. *et al.* Zwitterionic polymer ligands: an ideal surface coating to totally suppress protein-nanoparticle corona formation? *Biomaterials* **219**, 119357 (2019).

[21] van Andel, E. *et al.* Highly specific binding on antifouling zwitterionic polymer-coated microbeads as measured by flow cytometry. *ACS Applied Materials & Interfaces* **9**, 38211–38221 (2017). URL https://doi.org/10.1021/acsami.7b09725. PMID: 29064669, https://doi.org/10.1021/acsami.7b09725.

[22] He, M. *et al.* Zwitterionic materials for antifouling membrane surface construction. *Acta Biomaterialia* **40**, 142–152 (2016). URL https://www.sciencedirect.com/science/article/pii/S1742706116301349. Zwitterionic Materials.

[23] Sung, H. *et al.* Global cancer statistics 2020: Globocan estimates of incidence and mortality worldwide for 36 cancers in 185 countries. *CA: A Cancer Journal for Clinicians* **71**, 209–249 (2021).

[24] Miller, K. D. *et al.* Cancer treatment and survivorship statistics, 2019. *CA: A Cancer Journal for Clinicians* **69**, 363–385 (2019).

[25] El-Readi, M. Z. & Althubiti, M. A. Cancer nanomedicine: A new era of successful targeted therapy. *Journal of Nanomaterials* **2019**, 1–13 (2019).

[26] Estrella, V. *et al.* Acidity generated by the tumor microenvironment drives local invasion. *Cancer Research* **73**, 1524–1535 (2013).

[27] Fröhlich, E. The role of surface charge in cellular uptake and cytotoxicity of medical nanoparticles. *International Journal of Nanomedicine* 5577 (2012).

[28] Ou, H. *et al.* Surface-adaptive zwitterionic nanoparticles for prolonged blood circulation time and enhanced cellular uptake in tumor cells. *Acta Biomaterialia* **65**, 339–348 (2018).

[29] Hoshyar, N., Gray, S., Han, H. & Bao, G. The effect of nanoparticle size on in vivo pharmacokinetics and cellular interaction. *Nanomedicine* **11**, 673–692 (2016).

[30] Bai, Y. *et al.* Chemical control over cellular uptake of organic nanoparticles by fine tuning surface functional groups. *ACS Nano* **9**, 10227–10236 (2015).

[31] Hanlon, A. M., Lyon, C. K. & Berda, E. B. What is next in single-chain nanoparticles? *Macromolecules* **49**, 2–14 (2015).

[32] Kröger, A. P. P., Paats, J.-W. D., Boonen, R. J. E. A., Hamelmann, N. M. & Paulusse, J. M. J. Pentafluorophenyl-based single-chain polymer nanoparticles as a versatile platform towards protein mimicry. *Polym. Chem.* **11**, 6056–6065 (2020). URL http://dx.doi.org/10.1039/D0PY00922A.

[33] Kuhn, W. & Balmer, G. Crosslinking of single linear macromolecules. *Journal of Polymer Science* **57**, 311–319 (1962).

[34] Croce, T. A., Hamilton, S. K., Chen, M. L., Muchalski, H. & Harth, E. Alternativeo-quinodimethane cross-linking precursors for intramolecular chain collapse nanoparticles. *Macromolecules* **40**, 6028–6031 (2007).

[35] Harth, E. *et al.* A facile approach to architecturally defined nanoparticles via intramolecular chain collapse. *Journal of the American Chemical Society* **124**, 8653–8660 (2002).

[36] Kröger, A. P. P., Hamelmann, N. M., Juan, A., Lindhoud, S. & Paulusse, J. M. J. Biocompatible single-chain polymer nanoparticles for drug delivery—a dual approach. *ACS Applied Materials Interfaces* **10**, 30946–30951 (2018).

[37] Rothfuss, H., Knöfel, N. D., Roesky, P. W. & Barner-Kowollik, C. Single-chain nanoparticles as catalytic nanoreactors. *Journal of the American Chemical Society* **140**, 5875–5881 (2018).

[38] Perez-Baena, I. *et al.* Single-chain polyacrylic nanoparticles with multiple gd(iii) centres as potential mri contrast agents. *J. Mater. Chem.* **20**, 6916–6922 (2010). URL `http://dx.doi.org/10.1039/C0JM01025A`.

[39] Binder, W. H. & Sachsenhofer, R. 'click' chemistry in polymer and materials science. *Macromolecular Rapid Communications* **28**, 15–54 (2007).

[40] Li, Y. *et al.* Crosslinked dendronized polyols as a general approach to brighter and more stable fluorophores. *Chem. Commun.* **52**, 3781–3784 (2016). URL `http://dx.doi.org/10.1039/C5CC09430E`.

[41] Diou, O. *et al.* Rgd decoration of pegylated polyester nanocapsules of perfluorooctyl bromide for tumor imaging: Influence of pre or post-functionalization on capsule morphology. *European Journal of Pharmaceutics and Biopharmaceutics* **87**, 170–177 (2014).

[42] Gracia, R. *et al.* Synthesis and functionalization of dextran-based single-chain nanoparticles in aqueous media. *Journal of Materials Chemistry B* **5**, 1143–1147 (2017).

[43] Eberhardt, M., Mruk, R., Zentel, R. & Théato, P. Synthesis of pentafluorophenyl(meth)acrylate polymers: New precursor polymers for the synthesis of multifunctional materials. *European Polymer Journal* **41**, 1569–1575 (2005).

[44] Woodfield, P. A., Zhu, Y., Pei, Y. & Roth, P. J. Hydrophobically modified sulfobetaine copolymers with tunable aqueous ucst through postpolymerization modification of poly(pentafluorophenyl acrylate). *Macromolecules* **47**, 750–762 (2014). URL `https://doi.org/10.1021/ma402391a`. `https://doi.org/10.1021/ma402391a`.

[45] Wang, W., Ji, X., Kapur, A., Zhang, C. & Mattoussi, H. A multifunctional polymer combining the imidazole and zwitterion motifs as a biocompatible compact coating for quantum dots. *Journal of the American Chemical Society* **137**, 14158–14172 (2015). URL `https://doi.org/10.1021/jacs.5b08915`. PMID: 26465679, `https://doi.org/10.1021/jacs.5b08915`.

[46] Weinhart, M. *et al.* Linear poly(methyl glycerol) and linear polyglycerol as potent protein and cell resistant alternatives to poly(ethylene glycol). *Chemistry - An Asian Journal* **5**, 1992–2000 (2010).

[47] Zhu, H.-W. *et al.* Strong adhesion of poly(vinyl alcohol)–glycerol hydrogels onto metal substrates for marine antifouling applications. *Soft Matter* **16**, 709–717 (2019).

[48] Andel, E. V. *et al.* Systematic comparison of zwitterionic and non-zwitterionic antifouling polymer brushes on a bead-based platform. *Langmuir* **35**, 1181–1191 (2018).

6 Appendix

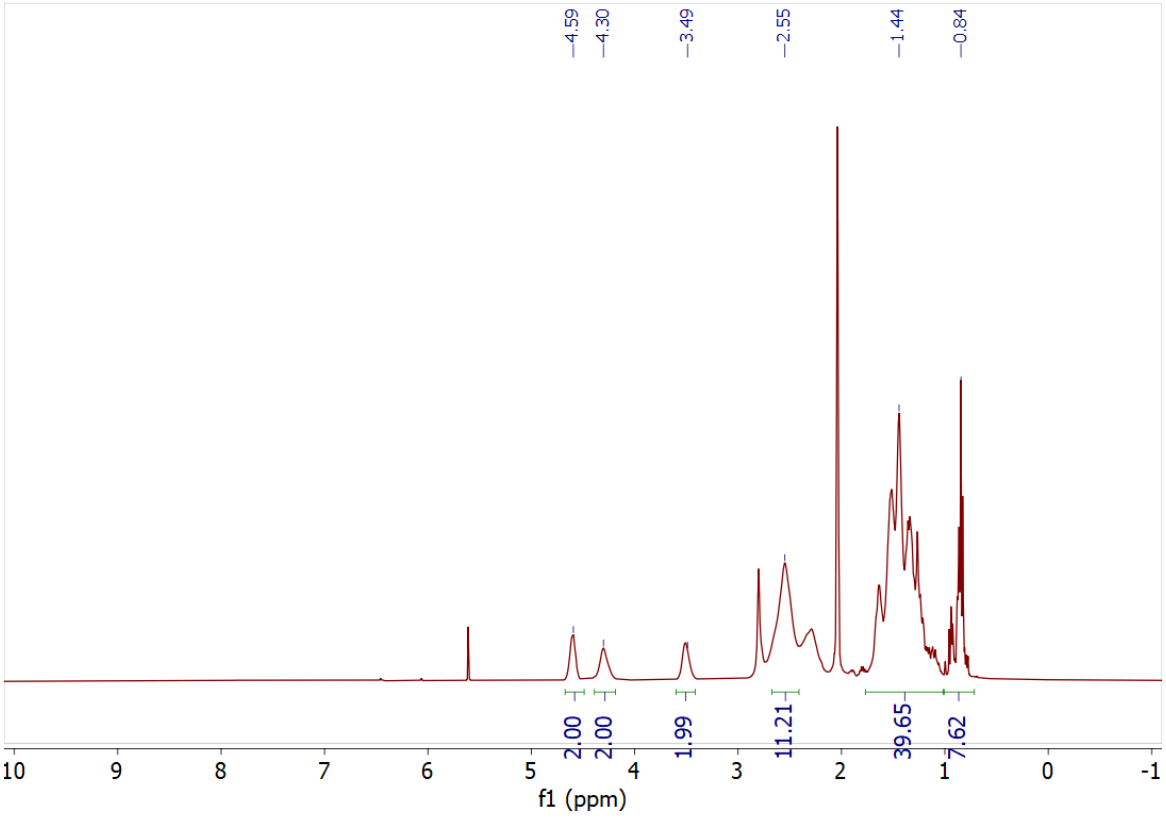

Figure 25: ^{1}H NMR of PFP-copolymer

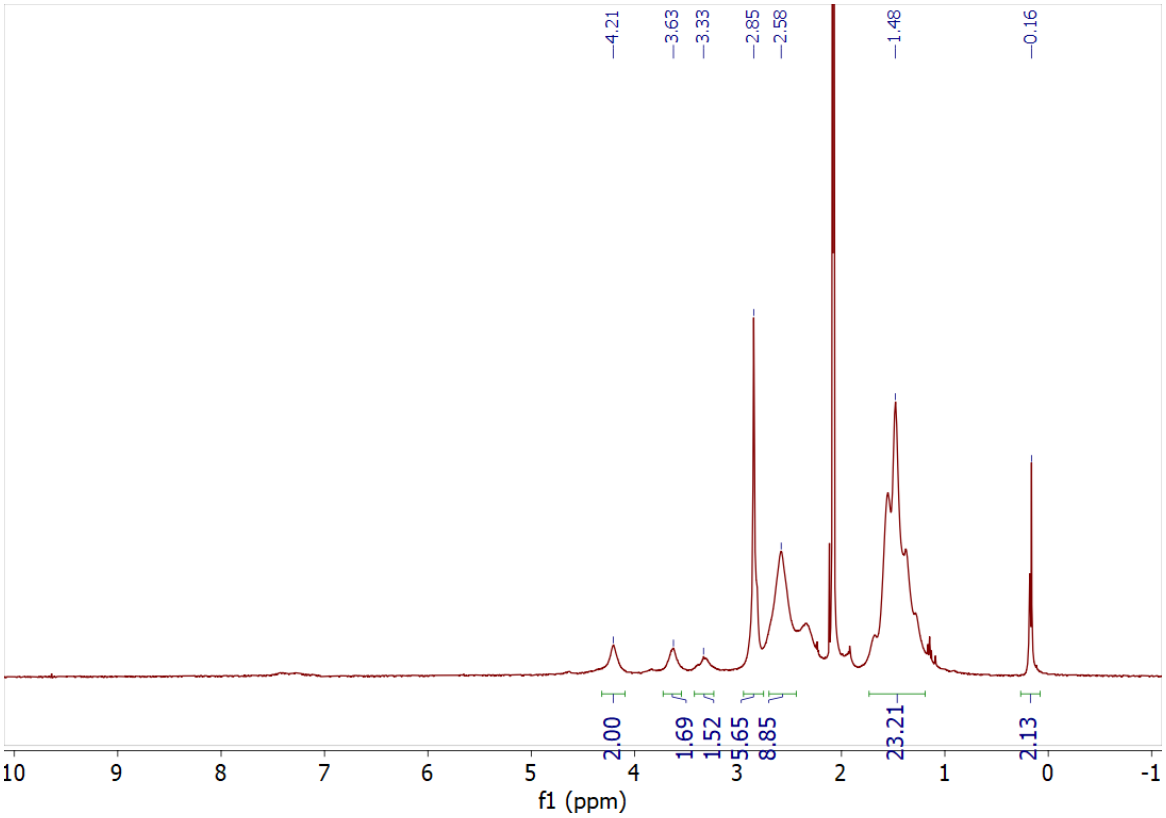

Figure 26: ^{1}H NMR of crosslinked PFP-SCNP

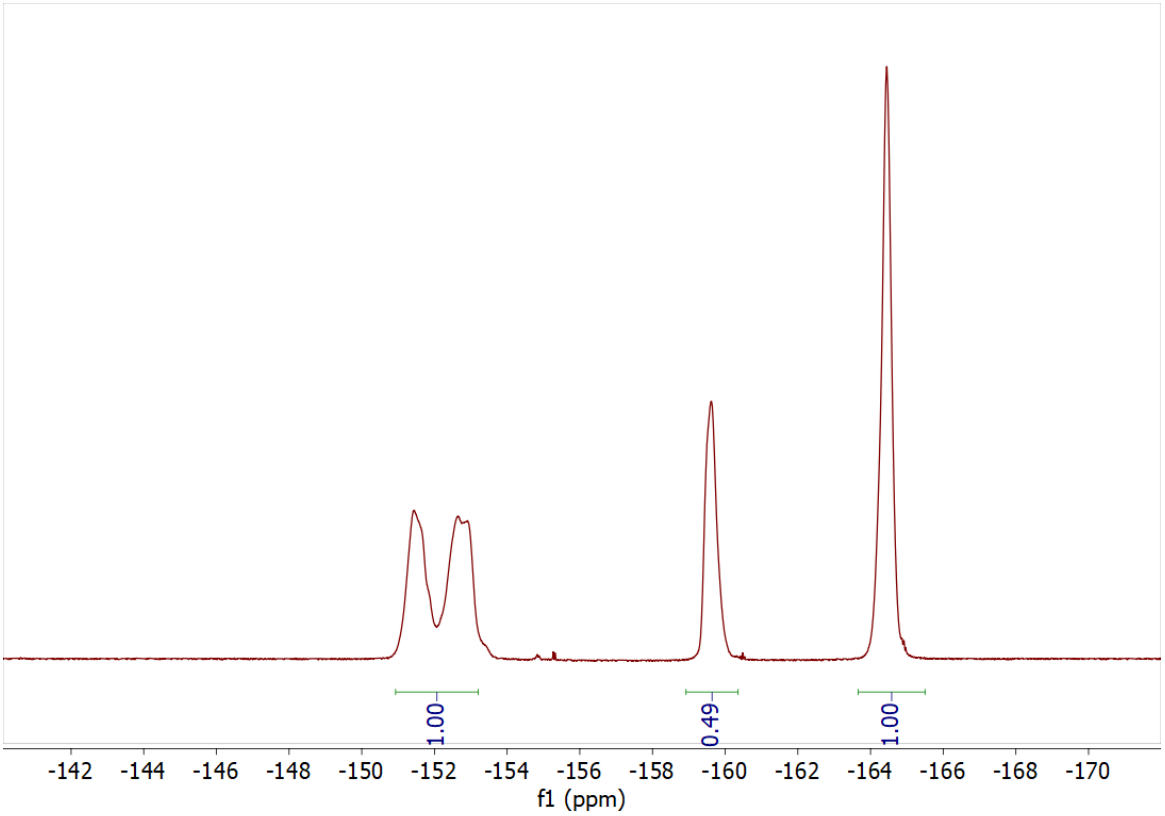

Figure 27: ^{19}F NMR of PFP-copolymer

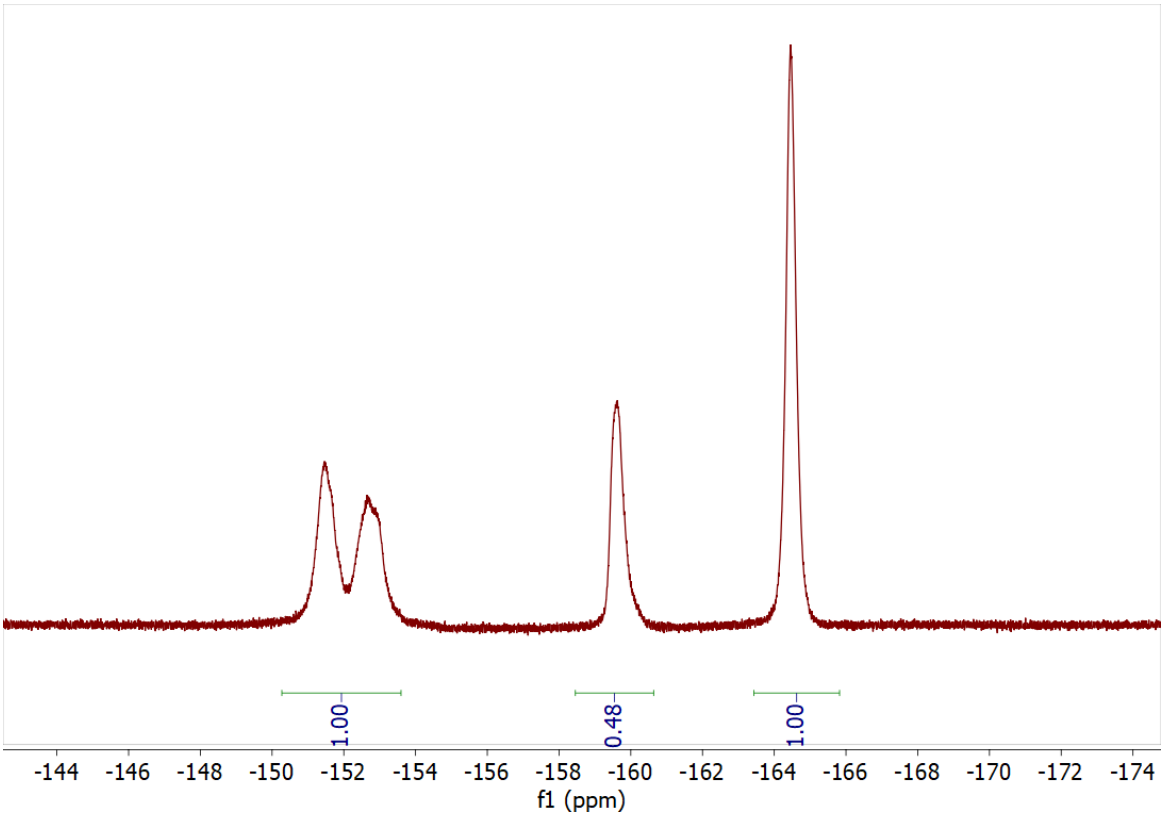

Figure 28: ^{19}F NMR of crosslinked PFP-SCNP

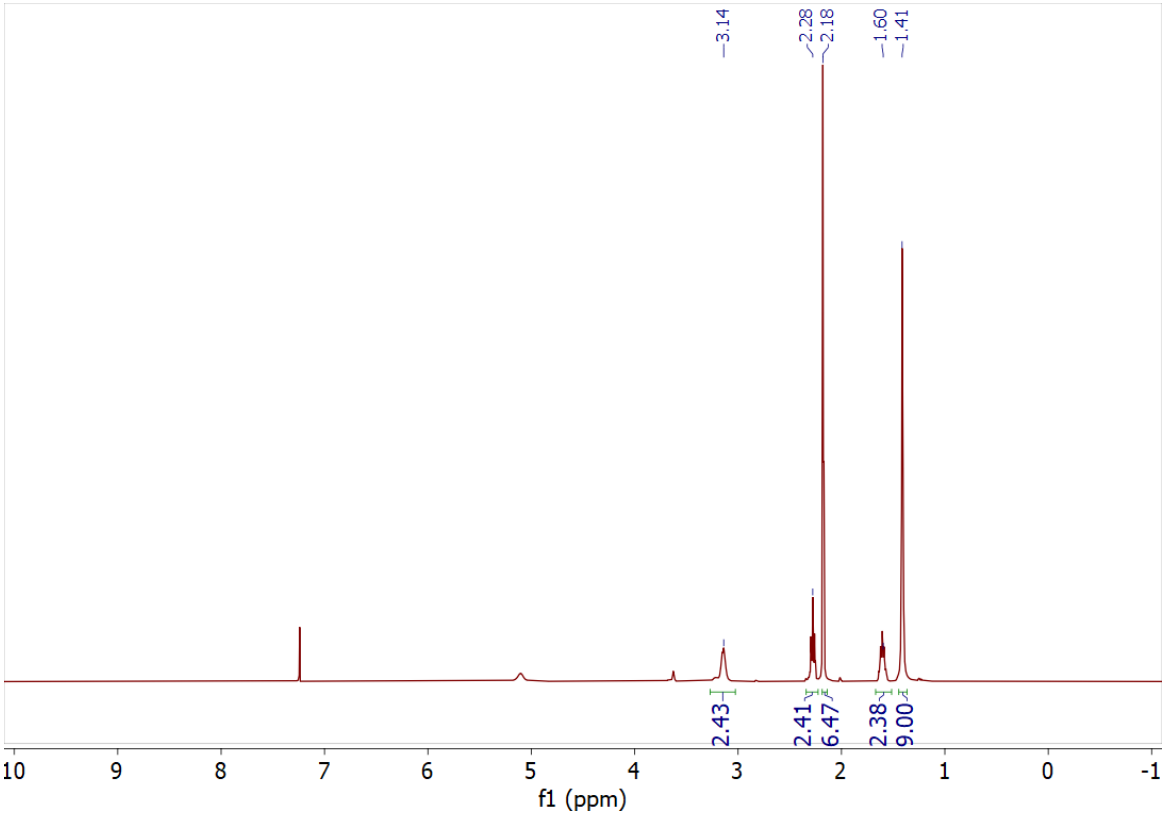

Figure 29: ^{1}H NMR of tert-Butyl (3-(dimethylamino)propyl)carbamate

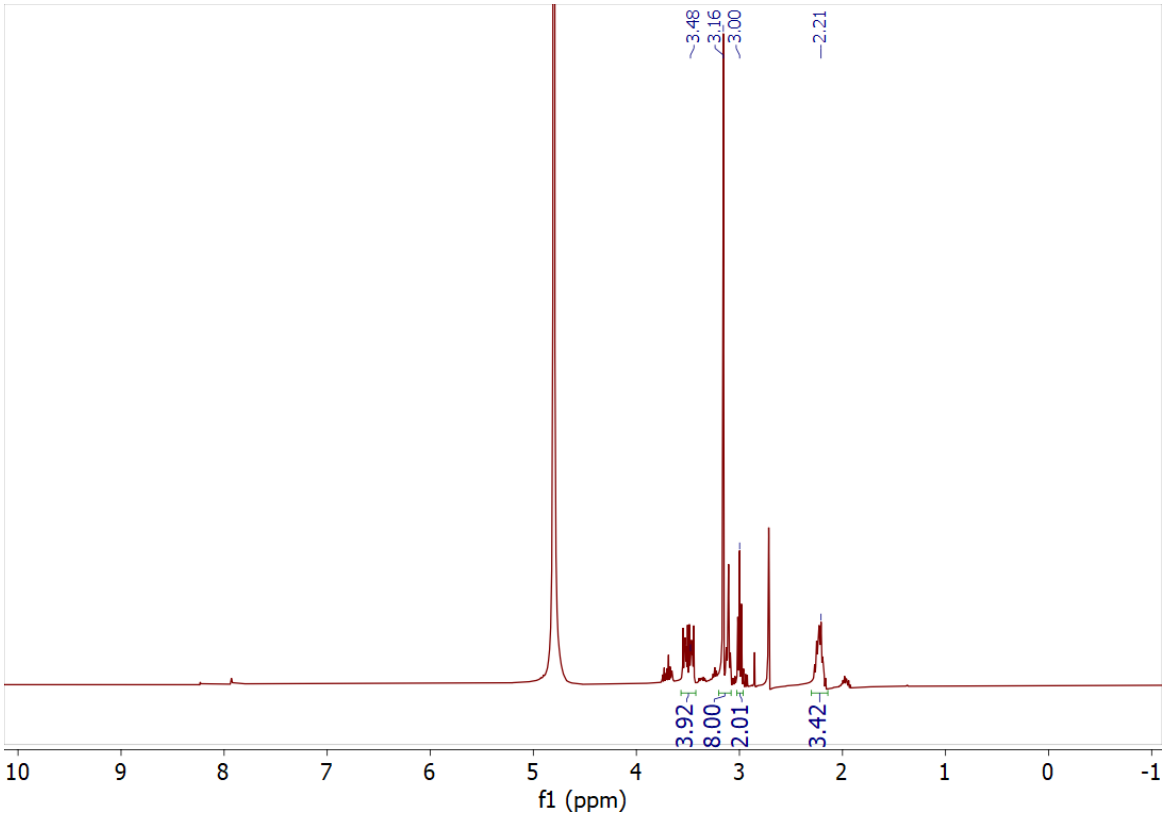

Figure 30: ^{1}H NMR of 3-((3-Aminopropyl)dimethylammonio)propane-1-sulfonate-HCL (ADPS-HCl)

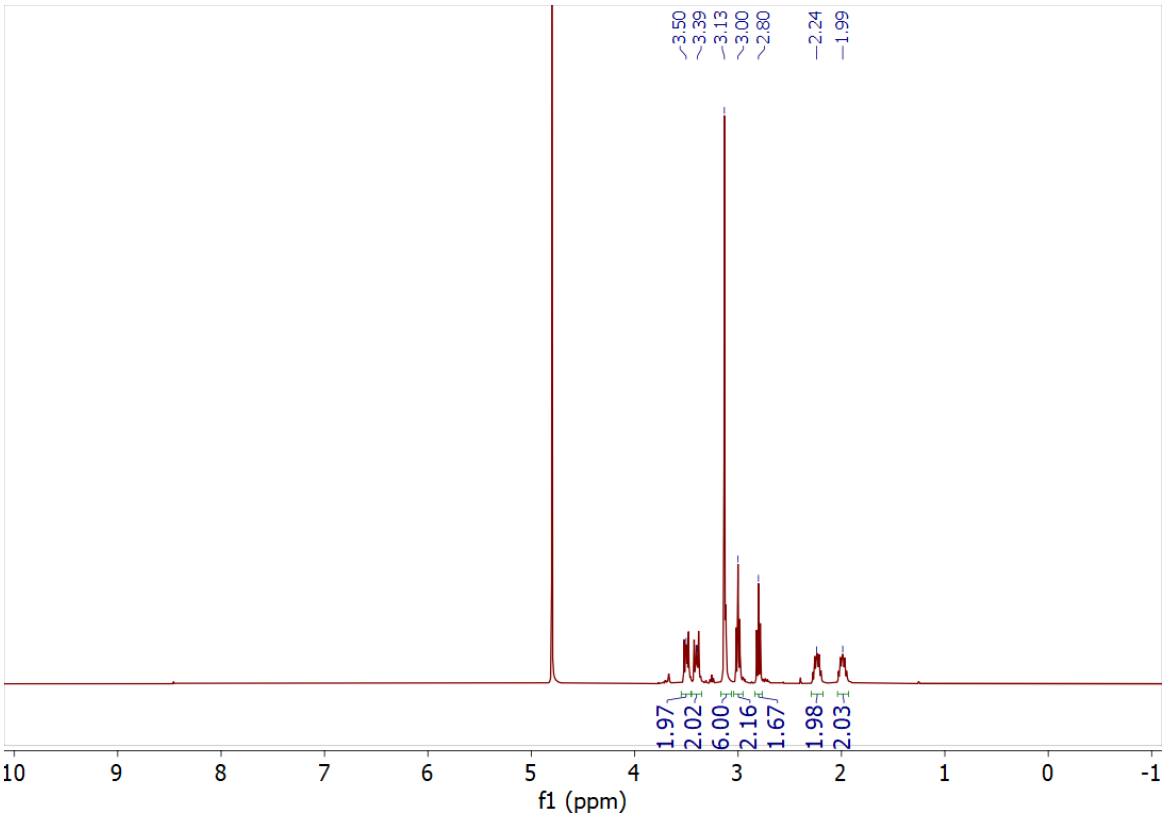

Figure 31: ^{1}H NMR of 3-((3-Aminopropyl)dimethylammonio)propane-1-sulfonate (ADPS)

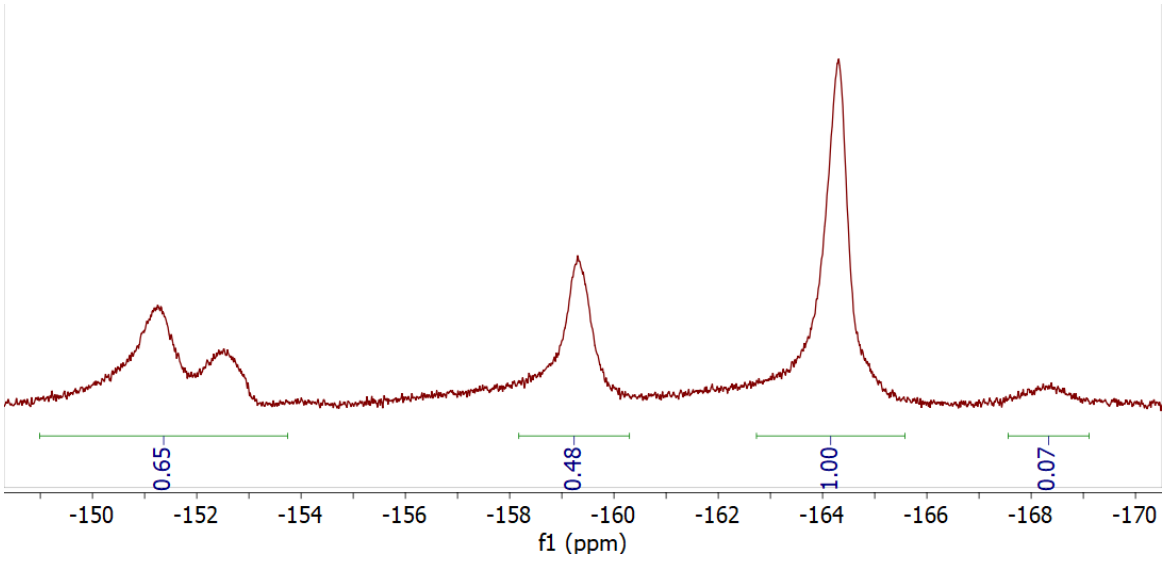

Figure 32: ^{19}F NMR of nanoparticle modified with APDS (0.2 eq)

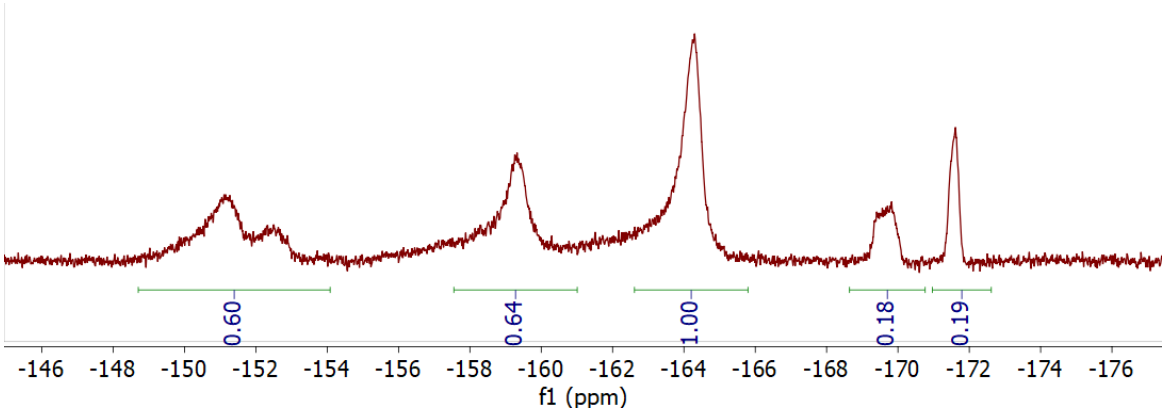

Figure 33: ^{19}F NMR of nanoparticle modified with APDS (0.4 eq)

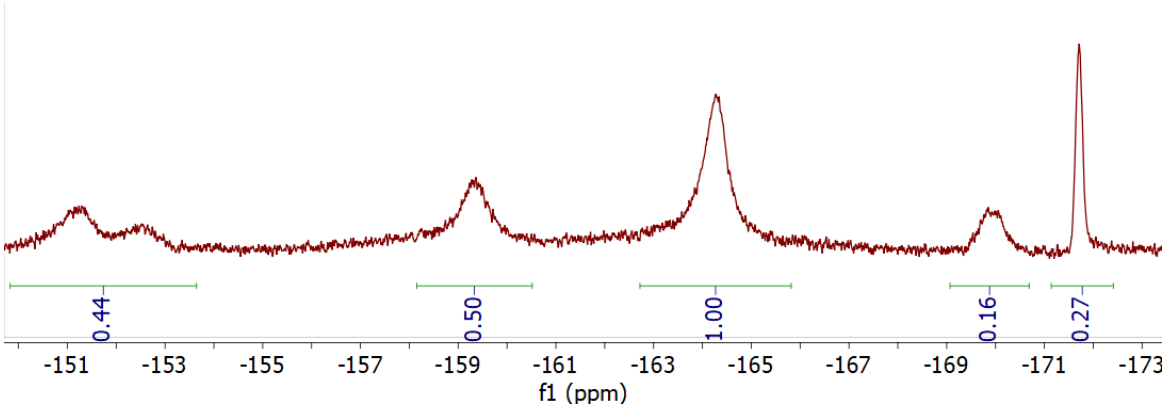

Figure 34: ^{19}F NMR of nanoparticle modified with APDS (0.6 eq)

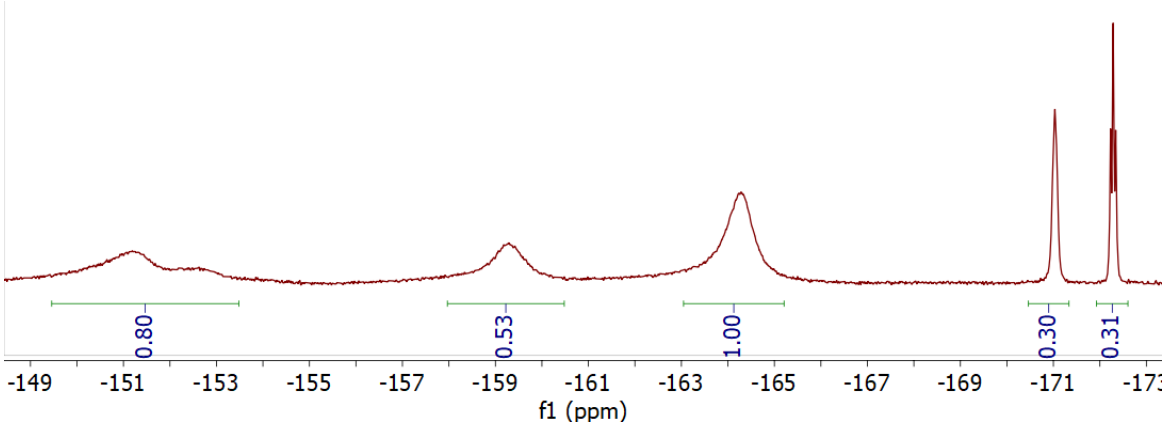

Figure 35: ^{19}F NMR of nanoparticle modified with histamine (0.1 eq)

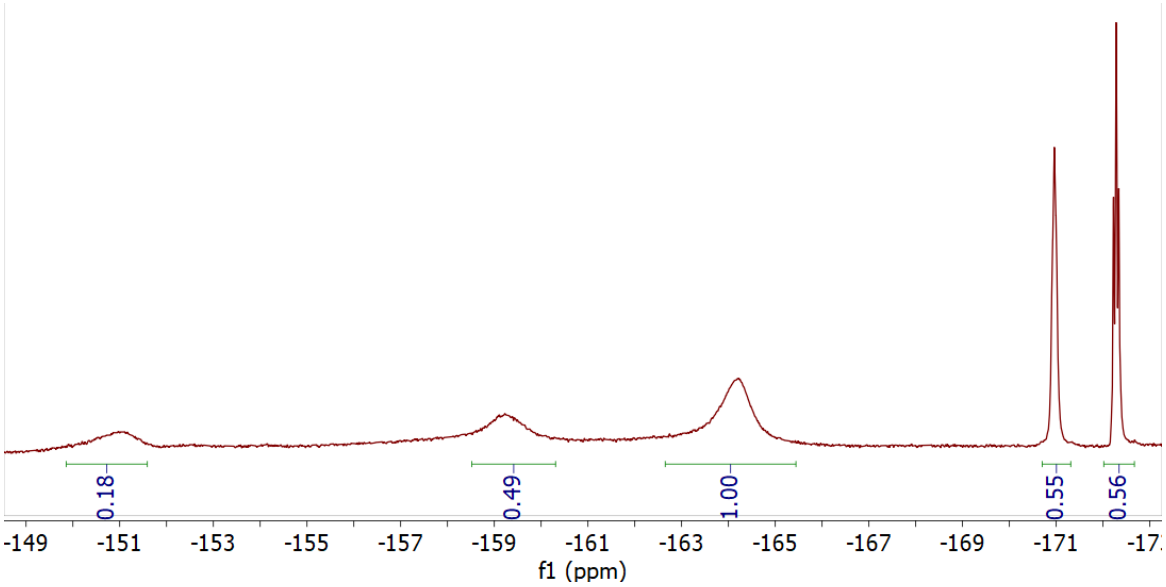

Figure 36: ^{19}F NMR of nanoparticle modified with histamine (0.3 eq)

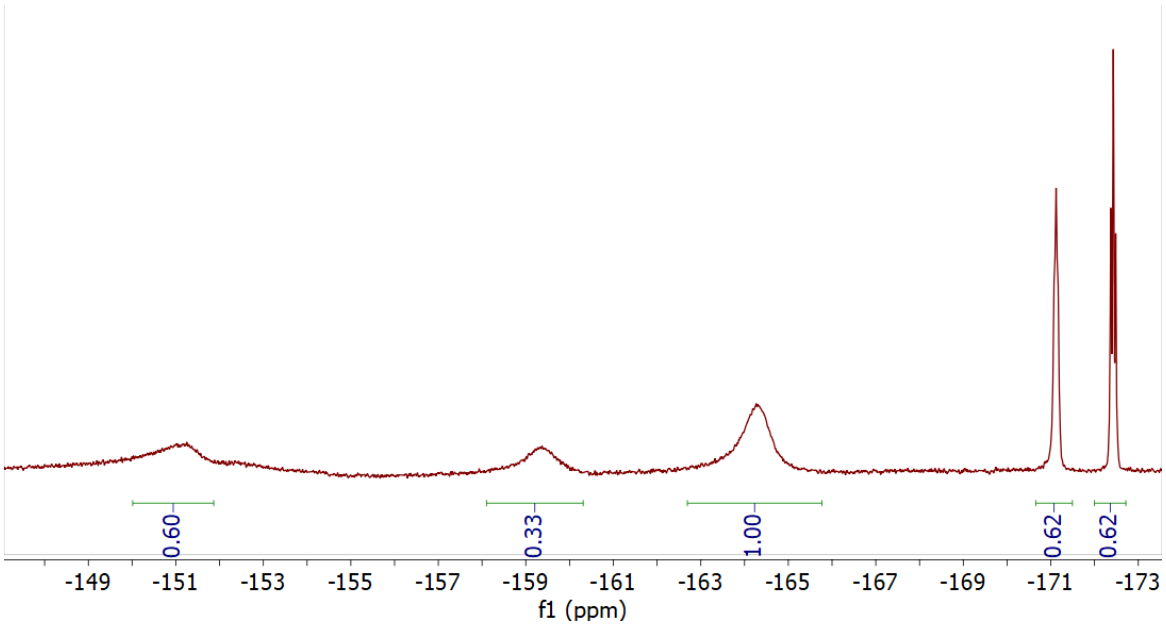

Figure 37: ^{19}F NMR of nanoparticle modified with histamine (0.5 eq)